LUND UNIVERSITY

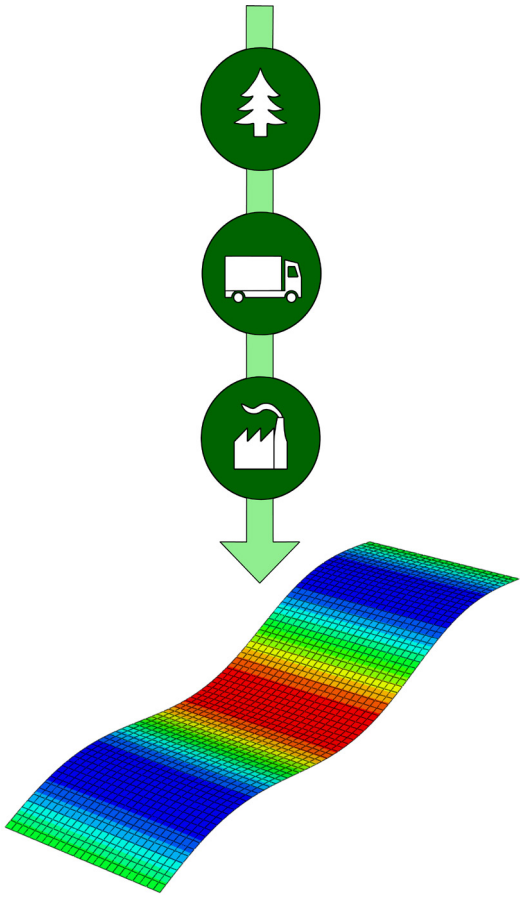

BALANCING BETWEEN ENVIRONMENTAL IMPACT AND VIBROACOUSTIC PERFORMANCE FOR LIGHTWEIGHT BUILDINGS

PHILIP CARLSSON

Structural Mechanics

Master's Dissertation

DEPARTMENT OF CONSTRUCTION SCIENCES
DIVISION OF STRUCTURAL MECHANICS

ISRN LUTVDG/TVSM--21/5253--SE (1-84) | ISSN 0281-6679
MASTER'S DISSERTATION

BALANCING BETWEEN ENVIRONMENTAL IMPACT AND VIBROACOUSTIC PERFORMANCE FOR LIGHTWEIGHT BUILDINGS

PHILIP CARLSSON

Supervisor: Dr **OLA FLODÉN**, Division of Structural Mechanics, LTH.
Assistant Supervisor: Dr **RIKARD SUNDLING**, Division of Construction Management, LTH
Examiner: Dr **PETER PERSSON**, Division of Structural Mechanics, LTH.

Printed by V-husets tryckeri LTH, Lund, Sweden, September 2021 *(Pl)*.

For information, address:
Division of Structural Mechanics,
Faculty of Engineering LTH, Lund University, Box 118, SE-221 00 Lund, Sweden.
Homepage: www.byggmek.lth.se

Abstract

Multi-storey buildings constructed in timber have become more common in recent years. A reason for this lies in the growing interest for sustainable building, where timber is seen as a particularly interesting alternative. As efforts have been made to improve the heat insulation in buildings, the energy consumption from manufacturing materials and from constructing buildings, referred to as embodied energy, accounts for an increasing proportion of the total energy consumption during the lifetime. Timber buildings offer an alternative for reducing the embodied energy as compared to traditional concrete buildings. However, timber buildings are more sensitive to low-frequency noise and vibrations, and studies have shown that exposure to high levels of noise and vibration increases the risk of anxiety, sleep disturbance and hearing loss. Consequently, this implies a balancing between embodied energy and noise and vibrations. This dissertation investigates such balancing when comparing timber buildings to traditional concrete buildings.

In this dissertation, different methods for calculating the vibroacoustic performance as a single scalar value are conducted in order to directly compare the vibroacoustic performance with the environmental impact of different choices of material. An LCA is conducted for the embodied energy and global warming potential of a CLT floor, a concrete-CLT composite floor, and a prestressed concrete floor using data provided by manufacturers and existing databases. Finite element models of the different floors are created, and the vibration levels are investigated for a unit load and footstep pulse. A parameter study is performed where the thickness of the CLT floor is varied. The different floors are compared in terms of vibroacoustic performance and LCA. Moreover, 2D finite element model of a ground with a building placed on top is created where the vibration levels are investigated for a unit load placed 20 m from the building to analyse the vibroacoustic performance due to an external load. The buildings investigated for external loading are a lightweight building with CLT floors or CLT-concrete composite floors, and a concrete building with prestressed concrete floors. A parameter study is performed for varying thicknesses of the CLT floors, and the buildings are compared for the vibroacoustic performance and LCA of the load-bearing structure.

The results show that the CLT floor and the composite floor has a higher vibration in relation to the concrete floor when exposed to an internal load. However, a seven-layered CLT floor with 50 mm ply thickness or a composite floor provides a relatively good vibroacoustic performance in relation to a concrete floor. The good vibroacoustic performance in the two aforementioned floors is more evident when evaluating the vibrations based on thresholds for human disturbance of vibrations. The CLT floors and the composite floor have a low global warming potential and a low non-renewable energy consumption compared to the concrete floor, while the total energy consumption is similar or higher than concrete due to energy demanding process of CLT manufacturing. A general trend is observed where an increase in the thickness of a CLT

floor improves the vibroacoustic performance. However, in some cases increasing the thickness resulted in a worse performance and the response proved to be sensitive to the walking frequency applied. The results suggest that when only considering absolute values, rather than thresholds, a good balance may be difficult to achieve as a very thick CLT floor would be required to achieve a similar vibroacoustic performance when exposed to an internal load.

The lightweight buildings have a lower vibration magnitude in relation to the concrete building when exposed to an external load, while having a lower global warming potential and use of non-renewable energy, but a higher total energy consumption. The results show that the response of the buildings is sensitive to the eigenfrequencies matching to the frequency content of the propagating ground waves making the optimal material selection very much specific to each case.

Sammanfattning

Flervåningsbyggnader konstruerade i trä har blivit alltmer vanliga de senaste åren. Anledningen till detta grundar sig ofta i det ökade intresset för hållbart byggande där trä ses om ett intressant alternativ. Förbättringar av värmeisoleringen i byggnader har gjort att energikonsumtionen vid byggskedet, den inbyggda energin, står för en alltmer större andel av en byggnads totala energikonsumtion. Träbyggnader erbjuder ett alternativ till en lägre inbyggd energi jämfört med traditionella betongbyggnader. Träbyggnader är dock känsligare mot lågfrekventa ljud och vibrationer. Långvarig exponering av höga nivåer av ljud och vibrationer har visat sig ge upphov till ökade risker för negativa effekter som exempelvis sömnproblem och hörselskador. Följaktligen antyder detta ett behov på en balans mellan inbyggd energi och vibroakustisk prestanda. Detta examensarbete undersöker denna balansering genom jämförelser mellan träbyggnader och betongbyggnader.

I detta examensarbete tillämpas olika metoder för beräkning av vibroakustisk prestanda som ett skalärt värde för olika material som direkt kan jämföras med dess miljöpåverkan. En LCA utförs för den inbyggda energin och globala uppvärmningspotentialen av ett CLT-golv, ett CLT-betong kompositgolv och ett golv av förspänd betong med data från existerande databaser. Finita elementmodeller av de olika golven skapas och vibrationsnivåerna undersöks för en enhetslast och en fotstegslast. En parameterstudie utförs där CLT-golvets tjocklek varieras. De olika golven jämförs med hänsyn till dess vibroakustiska prestanda och miljöpåverkan. Vidare skapas en 2D finita elementmodell över en mark med en byggnad placerad i mitten av modellen. En enhetslast placeras 20 m från fundamentets kant och byggnadens vibrationsnivåer undersöks i golven. Byggnaderna som undersöks är en lätt byggnad, främst bestående av trä med antingen CLT-golv eller kompositgolv, och en byggnad bestående av enbart betong med golv av förspänd betong. En parameterstudie utförs där CLT-golvens tjocklek varieras och de olika alternativens vibroakustiska prestanda och miljöpåverkan jämförs.

Resultaten visar att CLT-golvet och kompositgolvet har högre vibrationsnivåer jämfört med betonggolvet när det utsätts för interna laster. Ett kompositgolv, eller ett CLT-golv bestående av sju 50 mm tjocka lager gav dock en relativt god vibroakustisk prestanda i relation till ett 200 mm tjockt betonggolv. Den relativt goda vibroakustiska prestandan i dessa två golv visade sig ännu tydligare när jämförelser gjordes med hänsyn till gränsvärden baserade på vad människor uppfattar som störande. CLT-golven och kompositgolven hade en låg global uppvärmningspotential, och en låg förbrukning av icke-förnyelsebar energi. Den totala energikonsumtionen för dessa två golvtyper var dock likvärdig, eller högre än ett betonggolv. En trend kan observeras där en ökad tjocklek på CLT-golvet generellt leder till en ökad vibroakustisk prestanda. I vissa fall uppvisades dock en sämre vibroakustisk prestanda när tjockleken ökades och denna trend visade sig vara något känslig mot den tillämpade fotstegsfrekvensen. Detta resultat antyder att en god balans kan vara svår att uppnå för ett CLT-golv

eftersom ett mycket hög tjocklek krävs för att få en liknande vibroakustisk prestanda som ett betonggolv, om absoluta värden används som mått.

Den lätta byggnaden hade lägre vibrationsnivåerna oavsett vilket golv som användes, jämfört med betongbyggnaden. Den lätta byggnaden hade samtidigt en lägre GWP och förbrukning av icke-förnyelsebar energi, men en högre inbyggd energi. Resultaten visar även att byggnadens vibrationer är känsliga mot att dess egenfrekvenser matchar frekvensinnehållet i de propagerande markvågorna och medför att det optimala materialvalet blir specifikt för varje fall.

Acknowledgements

This Master's dissertation was performed at the Division of Structural Mechanics at the Faculty of Engineering, Lund University. I would like to thank my supervisor Dr Ola Flodén for his continuous guidance, input and ideas throughout the work. I would also like to thank my assistant supervisor Dr Rikard Sundling for his help and guidance for the LCA part of this dissertation. Lastly, I would like to thank my family for their continuous support, and my friends for the wonderful time I have had the past five years.

Philip Carlsson, 2021

List of abbreviations

LCA	Life cycle assessment
LCI	Life cycle inventory
LCIA	Life cycle impact assessment
EE	Embodied energy
PERE	Use of renewable primary energy (excluding renewable primary energy resources used as raw materials)
PENRE	Use of non-renewable primary energy (excluding non-renewable primary energy resources used as raw materials)
GWP	Global warming potential
AGWP	Absolute global warming potential
RF	Radiative forcing
PCR	Product category rule
EPD	Environmental product declaration
CLT	Cross-laminated timber
WBV	Whole-body vibration
FE	Finite element
FFT	Fast fourier transform
IFFT	Inverse fast fourier transform
VDV	Vibration dose value
VC	Vibration criteria
RMS	Root mean square
ERP	Equivalent radiated power
RSS	Root sum square
GRF	Ground reaction force

Contents

1 Introduction

1.1 Background

Following the ban on timber buildings exceeding two storeys which existed for over 100 years in Sweden and was not lifted until 1994, reinforced concrete and brick became the dominating materials used for construction of multi-storey buildings [1]. With this restriction being lifted, together with growing interest of sustainable building, construction of multi-storey buildings using timber has been growing in popularity in recent years as it is seen as a cheap and sustainable material.

It was reported by OECD [2] that the operational energy of buildings in 1999 accounted for over 40 % of the final energy consumption in the EU. Of the operational energy, space heating stood for 66 % in residential buildings. As efforts such as improved thermal insulation has been made during recent years, the energy consumption for construction and manufacturing of materials, referred to here as the *embodied energy*, has become increasingly important in relation to the total energy consumption of a building. In terms of global warming contribution, the production of concrete accounts for approximately 8.6 % of the global human-made CO_2 emissions [3].

Noise and vibration within the built environment is known to be a cause of disturbance. Regarding low frequency whole-body vibrations (WBV), claims of physiological effects such as sleep disturbance and anxiety have been made [4]. Sensitive equipment may also be negatively affected when exposed to vibrations. The vibrations may stem from within the building due to activity in adjacent rooms, for example footsteps and machinery. Vibrations may also stem from external sources such as nearby traffic. Noise in buildings is also known to be problematic and is related to vibrations as a vibrating element will emit noise. The embodied energy (EE), global warming potential (GWP) and vibroacoustic performance of a building depend on the design of the load bearing structure. It is therefore required in an early stage of design to predict the vibrations while taking into consideration the environmental impact in order to achieve a sustainable construction with sufficient vibroacoustic performance.

1.2 Aim and objective

The aim of this master's dissertation is to contribute with knowledge regarding prediction and evaluation of vibrations, noise, EE and GWP in an early stage of design of buildings, with focus on the balancing between these aspects. The objective is to establish a methodology in which both the vibroacoustic performance and the environmental impact can be quantified and directly compared with each other. A further objective is to evaluate the balancing between the different aspects when specifically comparing timber and concrete buildings.

1.3 Method

Values of EE and GWP for timber products and concrete is established. The EE and GWP are obtained from databases and environmental product declarations (EPD), both being based on life cycle assessments (LCA).

Through finite element (FE) analyses using Abaqus, the vibrational response of buildings is investigated and compared with the EE and GWP. This is performed for two different cases, the first one being a simply supported floor panel modelled in 3D subjected to a vertical load representing a source from within the building. The floor panel is the structural part of the floor acting as a foundation of the overlying layers and providing strength and stiffness. In addition to the floor panel, a floor is often composed of layers such as floor covering and soundproofing, which will not be modelled in this dissertation. The second case is a 2D-model of a building placed on soil. A vertical load is placed on the surface of the ground at a distance from the building representing an external source.

A parameter study is conducted for different floor panels and compared to concrete reference setups in two different cases. The floor panels investigated are a cross-laminated timber (CLT) panel with varying thickness and a CLT-concrete composite panel. The first case considers a floor panel exposed to either a unit load, or a footstep load based on experimental measurements found in literature. The reference floor for the first case is a prestressed concrete floor panel. The second case considers a three-storey building exposed to an external unit load placed at a distance from the building. The reference building for the second case is a building with all elements made of concrete.

With guidance from existing standards, different calculations of a scalar value reflecting the vibroacoustic performance is performed which is then compared with the EE and GWP. For these analyses, any trends in the balancing of vibroacoustic performance and environmental impact, in regards to the choice of material, are investigated.

1.4 Limitations

- Airborne noise is not investigated; only vibrations and their potential effect on structure-borne noise is considered.
- Only vibration velocities and accelerations transversal to the in-plane direction of building elements are considered.
- The EE and GWP is only considered for module A, i.e. the production and construction stage.
- Only the floor panel is modelled, i.e. effects of additional floor components are not considered.

1.5 Outline

- Chapter 2 contains an explanation of LCA and how these are evaluated in structures. The chapter also provides explanations of EE and GWP.
- Chapter 3 contains an overview of vibration- and noise transmission in buildings together with human perception. An overview of guidelines for evaluation and limitation of noise and vibration is also provided.
- Chapter 4 contains the governing theory of finite element calculations and structural dynamics.
- Chapter 5 presents the reference case of a floor panel exposed to an internal dynamic load together with the results from a parameter study.
- Chapter 6 presents the reference case of a ground model and a building exposed an external dynamic load together with results from the parameter study.
- Chapter 7 contains a discussion, conclusions and suggestions for future work.

2 Life cycle assessment

Life cycle assessment or life cycle analysis is a tool used to analyse the environmental impacts on a particular product or process through its entire life cycle. Figure 2.1 shows the procedure of an LCA where different stages of a building can be linked to different inputs and outputs [5]. This method allows stages of high impact to be identified allowing strategies for improvement to be employed.

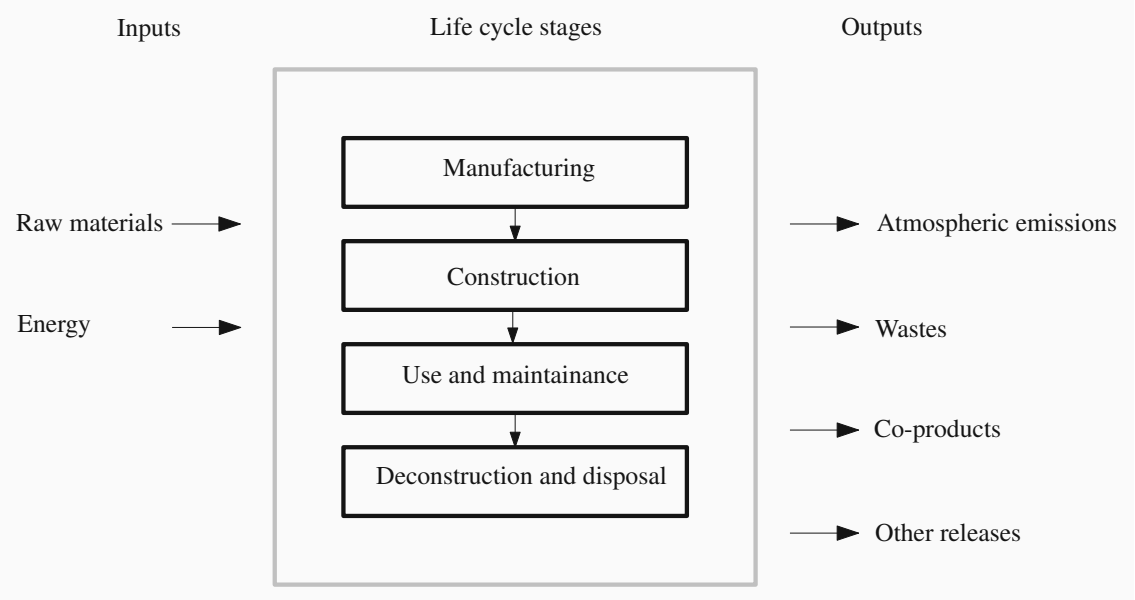

Figure 2.1: Inputs and outputs through the life cycle stages of a building.

2.1 Life cycle assessment in buildings

When considering buildings, LCA is used to evaluate the inputs and outputs of a whole building during its entire lifetime. The life cycle of a building consists of different stages, from construction and material use with its upstream production processes, through the operational stage to the end-of-life demolition. Each of these stages come with a specific resource use and environmental impact. Today, a range of standards exist for performing an LCA and evaluating the environmental impact of products and processes. These standards range from the fundamentals regarding environmental management systems and LCA, to more specific standards regarding environmental declarations of buildings and building materials [6]. Standardised product category rules (PCR) exist in SS-EN 15804 [7] for building products and SS-EN 15978 [8] for buildings. A PCR provides requirements on presented data and how it is presented and categorised. The different stages are in these standards divided into modules A–D describing parts of a life cycle. Following is a short description of the different modules given in SS-EN 15084:

- A: Product and construction stage, includes extraction of material, transport, manufacturing and assembly.
- B: Use stage, consists of the stage when the building is in use including all types of maintenance and refurbishments.
- C: End-of-life stage, includes any impact due to deconstruction into processing and disposal of the waste material.
- D: Benefits beyond the other stages such as reuse of material or recovery of energy stored.

In this dissertation, only module A is considered as it is at this stage the majority of the EE is accumulated. Analysis of the modules B, C and D requires extensive research into the operational demands of a building and the end-of-life procedures. Each stage is further divided into submodules providing more detailed accounting of the inputs and outputs. The submodules considered in this dissertation are the following:

- A1: Raw material supply
- A2: Transport (during manufacturing)
- A3: Manufacturing
- A4: Transport (to construction site)
- A5: Construction and installation

2.2 Assessment of data

Each of the life cycle stages often consist of multiple resource consuming processes such as transport, use of machines, or products used for manufacturing with the creation of by-products producing a range of inputs and outputs. All these processes need to be assessed and quantified for parameters such as energy use or GWP in order to achieve an accurate result.

The phase of quantifying different values is called life cycle inventory (LCI) and consists of analysing a process or product system in order to identify the inputs and outputs [5]. Gathering data for this may be difficult and time consuming for a specific case, and a simpler approach is to use existing databases. These databases consist of generic values often based on the average values for a specific country or region but may also exist for specific products. Since the impacts can vary significantly due to variations in factors such as transport distances, manufacturing processes and age of the data, this approach introduces a level of uncertainty which needs to be considered.

2.3 Environmental product declaration

An EPD is a declaration based on an LCA for a specific product which declares the environmental impact and resource use. An EPD is a convenient way of obtaining data on a specific product as it provides accurate data from the manufacturers in the modules A1–A3. In order to properly compare the different products, EPDs need to be performed using the same set of standards. The EPDs used in this report are performed in accordance with the standards ISO 14025, ISO 21930 and EN 15804. The reader is referred to these standards for a detailed explanation of the procedure used in the EPDs.

2.4 Environmental impact indicators

The environmental impact indicators are a set of values used in the life cycle impact assessment (LCIA). LCIA is a phase in an LCA where any inputs and outputs found in an LCI are evaluated and categorised for the environmental impact [9]. The environmental impact indicators are described as single equivalence values allowing a multitude of resource use and outputs to be quantified into singular values reflecting the area of environmental impact. The environmental impact indicators used in SS-EN 15804 are shown in Table 2.1. In this dissertation, only GWP is considered.

Table 2.1: Environmental impact indicators and units

Indicator	Unit
Global warming potential (GWP)	$kgCO_2 - eq.$
Depletion potential of the stratospheric ozone layer (ODP)	$kgCFC11 - eq.$
Acidification potential (AP)	$molH + -eq.$
Eutrophication potential (EP)	$kgPO_4 - eq.$
Formation potential of tropospheric ozone (POCP)	$kgNMVOC - eq.$
Abiotic depletion potential for non-fossil resources (ADPM)	$kgSb - eq.$
Abiotic depletion potential for fossil resources (ADPE)	MJ

2.5 Embodied energy

EE is defined as the primary energy consumed during the construction of a building [10]. EE is accumulated during different processes such as manufacturing of material, transport and on-site construction. EE is primarily evaluated for module A, but may include any additional energy consumption during processes such as refurbishment in module B, or transport during disposal of waste material in module C. The energy use is divided into primary and secondary energy use. The primary energy use consists of energy generated directly from natural resources such as, (according to EN 15804) coal, oil or wind. The secondary energy is extracted from later stages such as waste products, examples of secondary energy sources being solvents, wood or tyres. The energy demand for a product, presented as primary and secondary energy is also further

divided into renewable and non-renewable energy. In Table 2.2, the parameters used in terms of their abbreviation are shown with a short explanation of the definitions.

Table 2.2: Explanation of abbreviations used for energy demand in the dissertation

Abbreviation	Definition
PERE	Use of renewable primary energy
PENRE	Use of non-renewable primary energy

The operational energy use for buildings constructed in colder regions often stands for the majority of the total life cycle energy. As efforts have been made to reduce the operational energy through improved thermal insulation, heat recovery and reduced leakage, the proportion has shifted towards the EE being a more significant part of the total life cycle energy. Studies have shown that 40-60% of the total energy in some studied buildings was consumed in the production and construction stage [11].

2.6 Global warming potential

The GWP of a product is the environmental impact indicator that describes the combined effects a product or process has on global warming by the release of greenhouse gases. The most prevalent greenhouse gas contributing to global warming is carbon dioxide. Multiple gases contributing to global warming in various magnitudes exist, such as methane and nitrous oxide [5]. To summarise and compare the impact of all gases contributing to global warming, this environmental impact indicator is described using the unit kilogram carbon dioxide equivalent (kg CO_2-eq). This unit is defined as the radiative forcing (RF) caused by one kilogram of carbon dioxide, integrated over a certain time period, also called the absolute global warming potential (AGWP). The RF is a measurement of the change in energy flux in the atmosphere, where an increase of RF leads to higher temperatures [12]. The standard EN 15804 uses the time frame 100 years (GWP100), hereafter simply referred to GWP. The GWP of any other gas is expressed as the ratio between the AGWP for the considered gas and the AGWP for one kilogram of carbon dioxide. In Figure 2.2 a visualisation for the GWP of methane is shown, together with how it varies depending on the time horizon used.

When considering the GWP for timber, the values are presented as biogenic carbon, GWP_{bio}, and greenhouse gas, GWP_{ghg}. The biogenic carbon is presented as a negative value due to the trees storing carbon dioxide from the atmosphere [7]. This carbon dioxide is only stored during its lifetime as it is released when decomposed. The GWP_{ghg} can be considered as the net contribution to the GWP at the end of the life cycle which comes from the different processes during stages such as manufacturing and assembly.

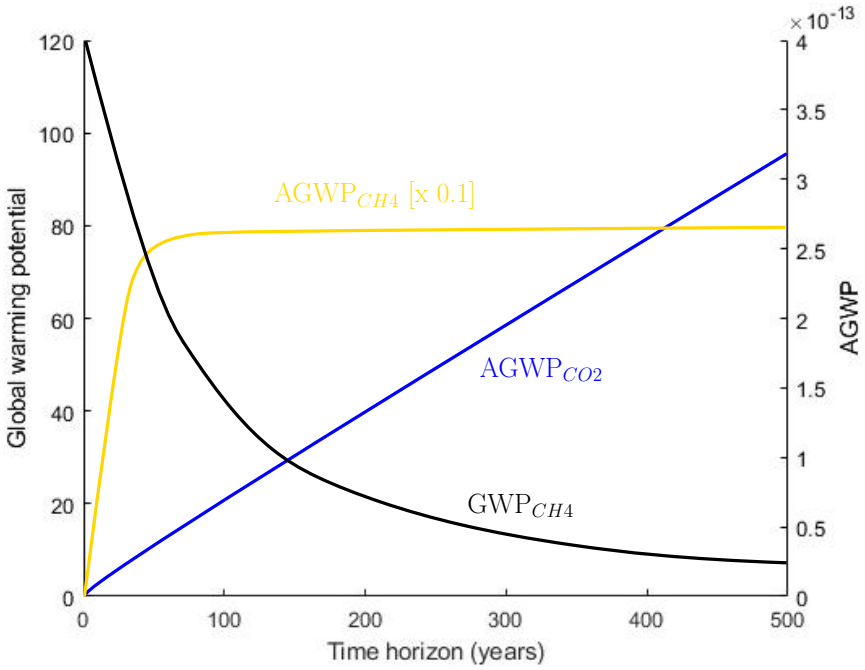

Figure 2.2: GWP of methane (black). The GWP is defined as the ratio between the AGWP of methane (yellow) and the AGWP of carbon dioxide (blue) [12].

2.7 Manufacturing of building materials

The building materials used in this report are prestressed reinforced concrete and CLT. In this section, an explanation of the manufacturing process is given with the underlying contributions and difference in regards to the environmental impact.

2.7.1 Cross-laminated timber

CLT is an engineered wood product consisting of individual boards held together by adhesive creating plenty of freedom in the dimensions of the panel. A CLT-panel often consists of an odd number of layers rotated 90-degrees in respect to each other, as seen in Figure 2.3. This creates a board with good strength characteristics.

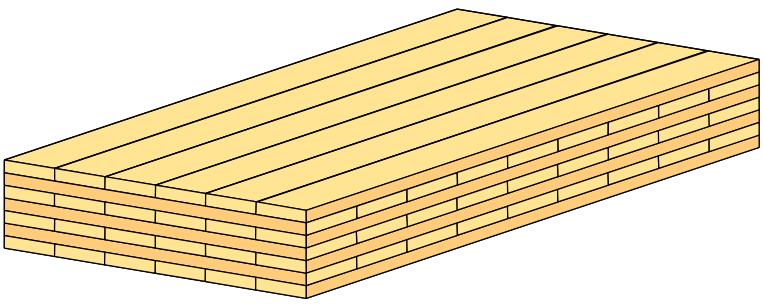

Figure 2.3: Visualisation of a seven-layered CLT-panel with colours indicating the orientation of the layers.

The production of CLT can be divided into three separate stages: resource extraction, lumber production and CLT production. The analysis of the resource use for CLT is taken from the LCA-report of Setra glulam [13] and is assumed to be similar for the production of CLT. The resource extraction for CLT consists of forestry with the main resource use being diesel used for harvesting and forwarding. The diesel consumption from forestry and transport is the main contributor to the non-renewable energy use and GWP_{ghg}. The lumber production consists of the process of creating sawn products from wood. This stage consists of processes such as debarking, sawing and drying. While this stage is often energy demanding, energy extracted from by-products during sawing is mainly used for drying making the external energy consumption low [6]. The lumber is then transported to the CLT-mill where the boards are created through gluing and pressing. The material input in this stage is wood and adhesive while also being energy demanding. The energy input in this stage does to a large extent consist of renewable sources in Sweden.

2.7.2 Reinforced concrete

Concrete is a very common construction material for multi-storey buildings characterised by high compression strength. In order to increase the tensile strength of concrete, it is often reinforced using steel. Reinforced concrete is a material manufactured using cement, aggregate, water and steel. The most significant contributor to energy use and GWP is the production of cement. The most common type of cement is Portland cement primarily consisting of limestone and silica. The raw material is milled to a fine powder and heated up to a temperature over 1400°C in a rotary where carbon dioxide is released in a process called calcination [14]. Achieving the high temperatures is a very energy demanding process often requiring fossil-fuels to be burned. An aspect not considered in this report is the carbonatation of concrete. Carbonatation is the process where concrete exposed to air decomposes, absorbing carbon dioxide from the atmosphere. Since the concrete in a building is not freely exposed to the air this process is slow and may be considered insignificant to the GWP [15]. The steel production in Sweden is mostly produced from iron ore where pig iron is created. The steel is produced by mixing the pig iron with coke and coal in a blast furnace, this process releases a large amount of carbon dioxide.

3 Noise and vibrations in buildings

Noise and vibrations in a built environment can stem from both external sources, such as traffic, and internal sources, such as footsteps. Long term exposure to high levels of noise and vibrations is known to be linked to health risks. In this chapter, fundamental theory of noise and vibrations in a built environment is presented. This chapter also provides theory regarding the human perception of noise and vibrations together with guidance on limits for acceptable levels.

3.1 Noise and vibration transmission

The transmission of noise and vibration can often be described separated into three different parts: source, medium and receiver. This is illustrated in Figure 3.1 from [16] and [17]. The three parts are described shortly in Sections 3.1.1–3.1.3.

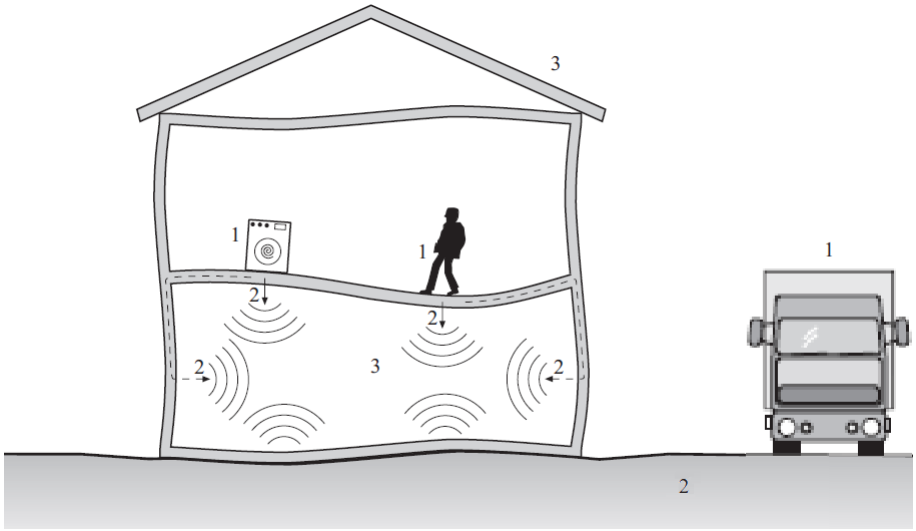

Figure 3.1: Illustration of source (1), transmitting medium (2) and receiver (3) in the transmission of noise and vibrations from internal and external sources.

3.1.1 Source

Vibrations and noises in the built environment can stem from both external and internal sources. External sources are located outside the building, examples being cars, trucks or rail traffic. These vibrations can, for example, be induced by irregularities in the asphalt layer or roughness of rails. The energy content of the vibrations also varies with the frequency with the highest energy content from railway traffic generally being below 20 Hz and from tram traffic being below 60 Hz [17].

Internal sources are vibrations that stem sources from within the building, examples being vibrating machinery and footsteps. In this dissertation, vibrations and noise due to footsteps i.e. a foot striking a floor, are investigated.

3.1.2 Medium

For external loads, the vibrations propagate through the ground, consisting of soil with underlying bedrock and other embedded objects such as bridges and tunnels. This makes the response at the receiving building dependant on the properties of the ground, and the resulting frequency spectra of the transmitted vibrations, which vary with the propagation distance.

3.1.3 Receiver

The receiver is the structure, person or object where the resulting noise and vibrations are evaluated. It is here that any limits in order to reduce negative effects are set. The limits can be based on human perception of vibration and noise, or by vibration criteria for sensitive equipment if the receiver is as such. Within a building, the transmission depends on factors such as material selection and geometry.

3.1.4 Noise transmission within buildings

Within acoustics, the transmission between rooms is distinguished between airborne sound transmission and structure-borne sound transmission based on the underlying mechanics of transmission.

- Airborne sound transmission is the type of transmission where sound is transmitted primarily with air as the medium. The transmission of sound occurs upon the sound waves impacting a building element, forcing it to vibrate with the energy being transmitted through the element [18] or penetrating any leakages. Typical sources of airborne sound is speech and speakers.
- Structure-borne sound is caused by impacts on building elements causing it to vibrate, resulting in transmission to adjacent rooms through connected elements.

In this report, structure-borne sound transmission is considered. The transmission to adjacent rooms occurs through multiple paths and is divided into direct transmission (D) through the separating element, and flanking transmission (F) through surrounding elements. In Figure 3.2 an illustration of the transmission paths is shown for airborne and structure-borne sound transmission [19].

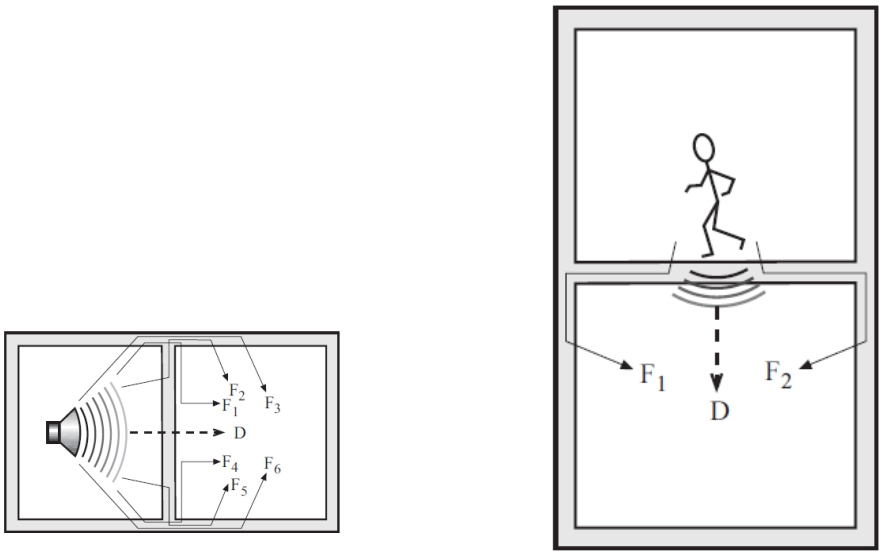

(a) Airborne sound transmission **(b)** Structure-borne sound transmission

Figure 3.2: Illustration of sound transmission types. D denotes a direct transmission path and F denotes a flanking transmission path.

The sound insulation performance of a building element is often measured using a weighted impact sound level or weighted sound reduction index. The evaluation of the performance of a building element is standardised in ISO 717-1 [20] and ISO 717-2 [21] for airborne sound insulation and impact sound insulation respectively by using a frequency domain reference curve of the sound level for impact sound and sound reduction for airborne sound. The evaluations performed in ISO 717 yields a singular value reflecting the sound insulation performance of a floor. This is performed by measuring the sound difference between adjacent rooms using a speaker for airborne sound and between adjacent storeys using a tapping machine for impact sound insulation.

3.2 Human perception and annoyance of noise and vibrations

Vibrations in buildings, and the noise induced by these vibrations can be a source of annoyance for residents and users. This is especially prevalent in lightweight buildings as the vibrational amplitudes often reach higher values. Studies performed in [22] have shown that impact sound is a source of annoyance in lightweight buildings despite having sufficient impact sound insulation according to standards. This was believed to be due to high levels of noise in the lower frequency range outside the scope of evaluation for impact sound insulation. A better correlation was found when an extended frequency range 20 Hz was used, rather than the limit of 50 Hz used in Swedish building codes.

3.2.1 Perception of sound

The frequency range in which humans are able the perceive sound, the audible spectrum, is generally regarded as 20 Hz–20 kHz and varies due to factors such as age. The subjective experience of a certain sound level depends on the frequency of the emitted sound. Rather than using narrow frequency bands, sound spectra are often presented in octave bands or one-third octave bands. The octave bands contain the sound energy at all frequencies between a lower bound frequency and an upper bound frequency. In this report, one-third octave bands are used with the centre frequencies being determined using base 2 calculations as:

$$f_c = 1000 \cdot 2^{n/3} \tag{3.1}$$

where n is a scalar representing the octave band. The upper frequency is calculated as:

$$f_u = f_c \cdot 2^{1/6} \tag{3.2}$$

Lastly, the lower frequency bound is calculated as:

$$f_l = f_c / 2^{1/6} \tag{3.3}$$

To account for the frequency-dependant experience of sound, weighting spectra are usually applied to the sound spectra depending on the application. A-weighting is a common weighting used to describe the apparent loudness a human would experience which is because humans are less sensitive to the lower and higher frequencies within the audible spectrum. In addition to A-weighting, C- and Z- weighting are commonly used, the weightings being shown in Figure 3.3. The Z-weighting is a flat filter with zero gain in all frequencies while the C-filter is a similar weighting to A with a lower attenuation in the lower frequencies. C-weighting is used to evaluate the sound emissions of certain machines and for peak noise measurements as the response of a human is flatter at higher sound levels.

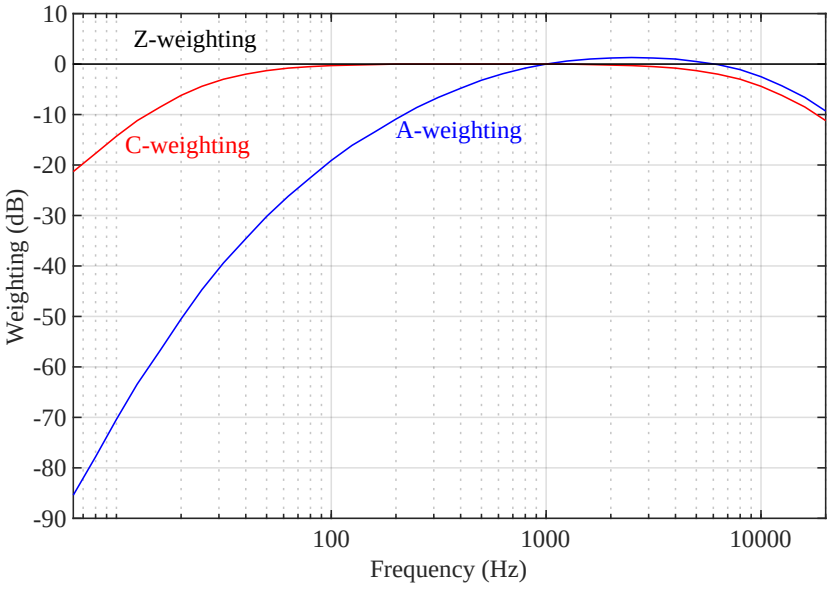

Figure 3.3: A-, C- and Z- weighting filters for noise.

3.2.2 Whole-body vibrations

In addition to discomfort, studies have shown evidence that exposure to WBV, being vibrations within the frequencies 1 Hz–80 Hz, is linked to health risks. Long term exposure of WBV is stated in ISO 2631-1 [23] to affect the lumbar spine and the connected nervous system. While the effects apply to any WBV, it is more prevalent for intense vibrations found in vehicles, for example, rather than buildings. It is assumed that an increase in the vibration dose, linked to exposure time and intensity further increases the risks.

As with noise, humans have a varying sensitivity to WBV depending on the frequency content of the vibration. Furthermore, the disturbance depends on the use of the building with varying sensitivity for room types such as laboratories, offices and workshops. To account for the frequency-dependence of the human sensitivity, weighting spectra may be applied to the vibrations. This frequency weighting is described in standards such as ISO 2631 and BS 6841 using the measured acceleration [24].

In this dissertation, the frequency weighting curve given in ISO 2631-2 [25] is used which gives a frequency weighting for WBV within the frequencies 1 Hz–80 Hz. The standard describes a transfer function $|H(p)|$ calculated from the product of the high-pass filter $|H_h(p)|$, low-pass filter $|H_l(p)|$ and a pure weighting function $|H_t(p)|$. The transfer function gives the frequency weighting W_m shown in Figure 3.4 which the unweighted acceleration spectra are multiplied with. $|H_h(p)|$ is given by

$$|H_h(p)| = \sqrt{\frac{f^4}{f^4 + f_1^4}} \tag{3.4}$$

where $f_1 = 10^{-0.1}$ Hz. $|H_l(p)|$ is given by

$$|H_l(p)| = \sqrt{\frac{f_2^4}{f^4 + f_2^4}} \tag{3.5}$$

where $f_2 = 100$ Hz. $|H_t(p)|$ is given by

$$|H_t(p)| = \sqrt{\frac{f_3^2}{f^2 + f_3^2}} \tag{3.6}$$

where $f_3 = \frac{1}{0.028 \cdot 2\pi}$ Hz. Lastly, the transfer function of the frequency weighting, W_m is given by

$$H(p) = H_h(p) \cdot H_l(p) \cdot H_t(p) \tag{3.7}$$

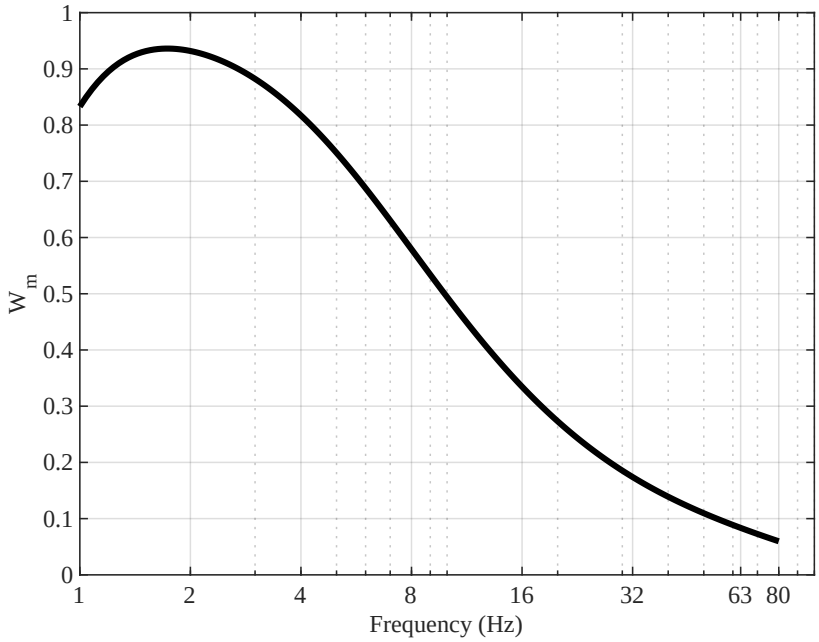

Figure 3.4: Weighting spectrum within frequencies 1 Hz – 80 Hz as given by ISO 2631-2.

In this dissertation, the weighting spectrum is used to evaluate the vibration response due to footsteps by multiplying the frequency spectra for accelerations with the weighting spectrum. For calculations of a weighted vibration dose value (VDV) in the time domain, see description of VDV in Section 4.5.2, the response is transformed into the frequency domain using a fast fourier transform (FFT) where the weighting is applied. The response is then transformed back to the time domain using an inverse fast fourier transform (IFFT) resulting in a filtered time signal as shown in Figure 3.5.

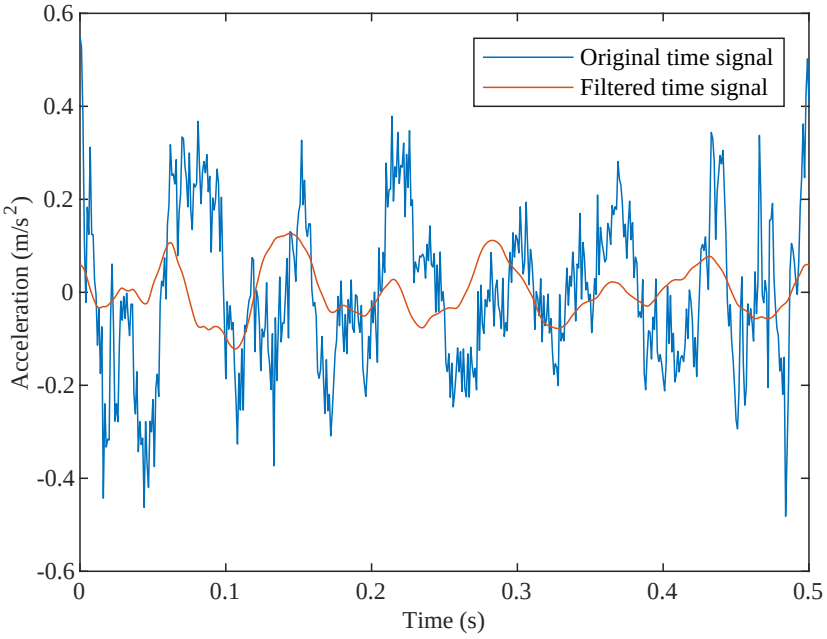

Figure 3.5: Filtered time signal using FFT, weighting spectrum and IFFT.

3.2.3 Guidance on limitations for noise and vibrations

There are currently no clear limits on WBV with regards to human health and comfort stated due to the complexity of the human response. Some guidance on vibration criteria is found for the serviceability limit state in ISO 10137:2008 [26] with the base curve levels shown in Figure 3.6. The base curve provides a spectrum on the acceleration, weighted according to ISO 2631-2 as shown in section 3.2.2, where the acceleration is considered satisfactory in regards to WBV. This base curve is adjusted using multiplying factors depending on room type, time of day, and occurrences of vibration. In this report the multiplying factor 2, which corresponds to an office or residential building during daytime, is used.

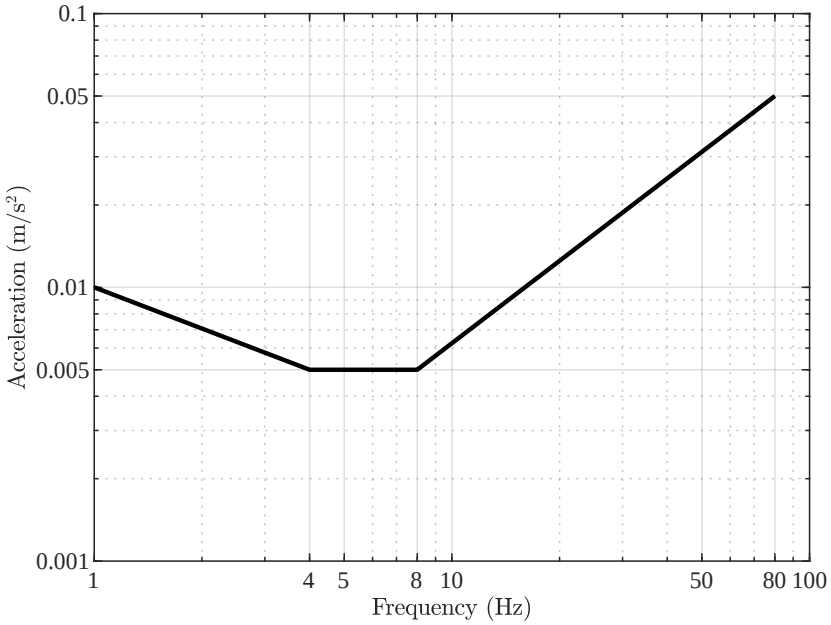

Figure 3.6: Base curve for building vibration in foot-to-head direction according to ISO 10137:2008.

The following background to guidance on noise and vibrations in buildings is not employed in this dissertation, but is included to provide a broader overview. The standard ISO 10137:2008 provides some probability limits for adverse comments in terms of VDV. Presented in Table 3.1 are thresholds with different probabilities of adverse comments in residential buildings, measured for 16 hours during daytime, or 8 hours during night-time. The standard suggests that if the ratio between the peak value and the RMS value of the filtered acceleration is greater than 6, using the VDV may be more appropriate.

Table 3.1: VDV ($m/s^{1.75}$) thresholds for probability of adverse comments in residential buildings.

Time of day	Low probability	Possible	Probable
16 h day	0.2-0.4	0.4-0.8	0.8-1.6
8 h night	0.13	0.26	0.51

Disturbances due to vibrations in the low-frequency range have been shown to occur at velocities just slightly above the perception level. The standard SS 4604861 provides a threshold for moderate disturbance being frequency dependant and occurring at lower velocities for frequencies above 8Hz.

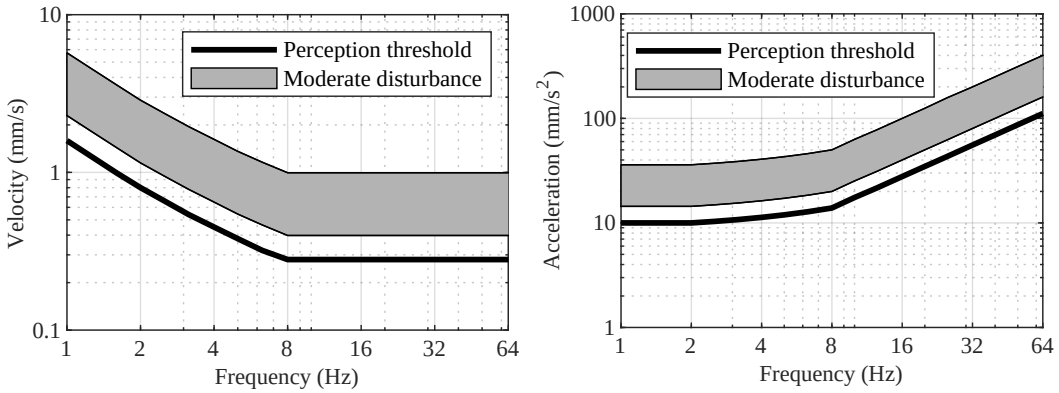

(a) Velocity threshold for perception and moderate disturbance.

(b) Acceleration threshold for perception and moderate disturbance.

Figure 3.7: Thresholds for perception and moderate disturbance due to vibrations according to SS 4604861.

Vibration criteria (VC) curves have been developed giving generic frequency dependant RMS velocity limits depending on the sensitivity of the applied area. The limits provided in the VC curves can give some reasonable limits for spaces varying from non-sensitive areas such as workshops to extremely sensitive areas such as research spaces with highly sensitive equipment.

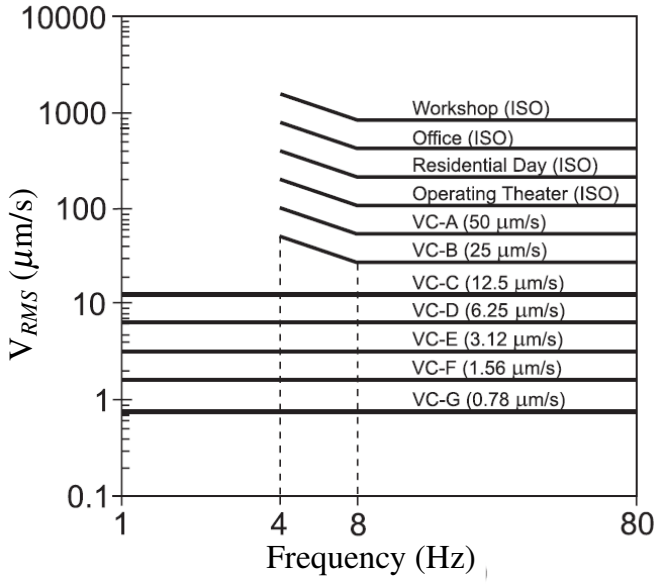

Figure 3.8: Vibration criteria curves [17].

In regards to impact noise, the Swedish standard SS 25267:2015 [27] provides a classification system for dwellings ranging from A–D depending on the ability of a separating

floor to insulate sound. The standard uses the standardised single values provided in ISO 717-2 [21] to determine the sound class. Boverket's building regulations sets a threshold outside the standard where the impact sound pressure level is considered sufficient in regards to annoyance of residents in a dwelling. The thresholds found in SS 25267:2015 and Boverket's building regulations is presented in Table 3.2.

Table 3.2: Sound classification thresholds in dwellings according to SS 25267:2015 [27].

Sound class	A [dB]	B [dB]	BBR [dB]	D [dB]
Weighted standardised impact sound pressure level, $L_{nT,w,50}$	48	52	56	60

The value $L_{nT,w,50}$ is calculated by placing a tapping machine on a floor and measuring the sound level in the adjacent room separated by the floor. $L_{nT,w}$ is calculated by shifting the reference curve provided in ISO 717-2 to the measured sound spectrum within the octave band centre frequencies 100 Hz–3150 Hz. $L_{nT,w,50}$ is determined by adding a spectrum adaptation term considering the octave band centre frequencies 50 Hz – 2500 Hz. Sound classifications A–D exist in SS 25268:2007 [28] for other types of rooms such as educational rooms, preschools or office work rooms with thresholds set depending on area of measurements and acoustical loading.

3.3 Calculation of scalar values for vibroacoustic performance

Different scalar values representing the vibroacoustic performance are calculated in this dissertation. In this section, the procedure used for calculating the scalar values is presented. For the footstep load, the RMS of the acceleration spectra in the frequency-domain is calculated. Further, the exceedance of the base curve presented in Figure 3.6, and the VDV is calculated. The procedure for calculating the VDV and base curve exceedance is schematically presented in Figure 3.9.

To apply the base curve to the response from footsteps, an FFT is performed on the time-signal where the weighting spectrum shown in Section 3.2.2 is used. The weighted narrow band spectrum is converted into 1/3 octave bands and an average acceleration from several different footstep walking frequencies is calculated. The scalar value reflecting the vibrational performance in regards to the base curve is calculated as the root sum square (RSS) of the exceedance of the base curve in the 1/3 octave bands. The exceedance of the base curve is the difference between the acceleration and the corresponding base curve acceleration in each 1/3 octave band; an acceleration below the base curve value has an exceedance equal to zero.

The VDV is calculated for footstep loading using the procedure presented in Section 3.2.2. The time length used for the VDV calculations in this report is the time period between two consecutive footsteps.

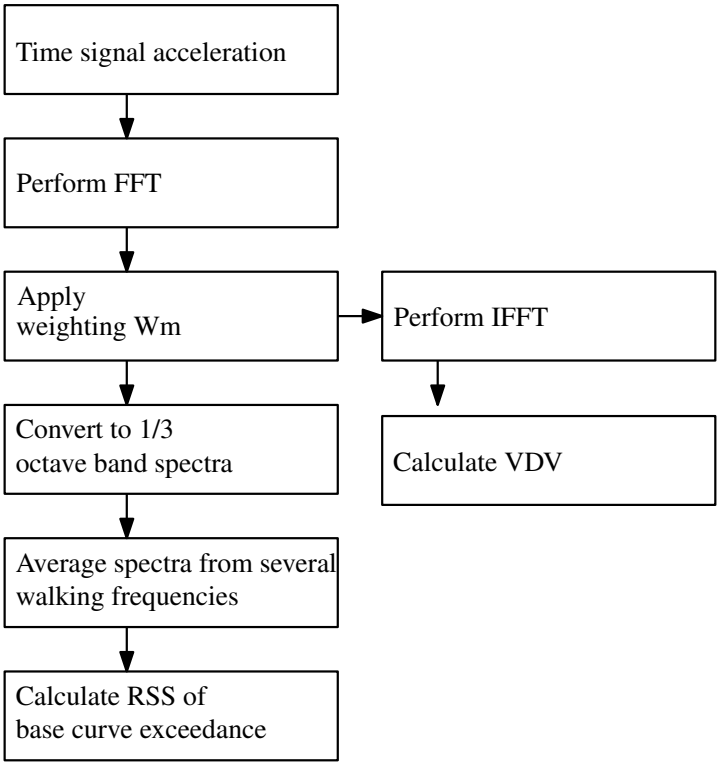

Figure 3.9: Procedure for calculating VDV and base curve exceedance of footstep loading.

Furthermore, calculations of scalar values without reference to limits found in standards is used for the analyses with a unit load in the frequency domain (which is equivalent to an impulse response in the time domain). The FRF of the velocity is used to calculate a velocity RMS value and the equivalent radiated power (ERP). The FRF of the acceleration is also used for calculating an acceleration RMS value. For an explanation of VDV, RMS and ERP, see Section 4.5.

4 Governing theory

In this chapter, an overview of the theory regarding FE modelling and structural dynamics is presented. The presented theory is based on the assumption of linearity.

4.1 Finite element method

The FE method is used to numerically solve partial differential equations. In the FE approach, a mesh is created by dividing the geometry into smaller, finite elements. For each element, a field variable is calculated using shape functions to approximate the spatial dependence. Within each element, a number of nodes exist depending on whether a linear, quadratic or any higher order polynomial of the shape function is used. These nodes are assigned discrete values. The FE method provides an approximation to the partial differential equation and can be used to construct the system matrices in the equation of motion in 4.2. With smaller element sizes, and an increased amount of elements, the solution converges towards an exact value at a higher computational cost. More detailed description of the finite element formulation can be found in literature such as [29].

4.2 Structural dynamics

The simplest way to describe a dynamic system is to consider a single degree of freedom (sdof) system. By introducing a dynamic load, $p(t)$ and considering the resisting forces, the equation of motion can be given through Newton's second law of motion. This system is loaded by the time-dependent dynamic force and consists of a mass, m, a damper, c, and a spring, k, expressed as:

$$m\ddot{u} + c\dot{u} + ku = p(t). \tag{4.1}$$

For a system with multiple degrees of freedom (mdof), Equation 4.1 is expanded to a system of equations. This set of equations can be described in matrix form using the mass matrix, $\mathbf{M}$, the damping matrix, $\mathbf{C}$, and the stiffness matrix, $\mathbf{K}$:

$$\mathbf{M\ddot{u}} + \mathbf{C\dot{u}} + \mathbf{Ku} = \mathbf{p}(t). \tag{4.2}$$

4.2.1 Eigenvalue analysis

An eigenvalue analysis provides the natural frequencies and modes of a system. An undamped free mdof system, i.e. a system not subjected to any external forces can be written as

$$\mathbf{M\ddot{u}} + \mathbf{Ku} = 0. \tag{4.3}$$

The displacement amplitude of Equation 4.3 can be described as the time dependant function

$$\mathbf{u} = \mathbf{\Phi} sin(\omega t). \tag{4.4}$$

Where $\mathbf{\Phi}$, is a vector that does not vary with time, and ω is the angular frequency. Inserting Equation 4.4 into Equation 4.3 yields the following expression:

$$(\mathbf{K} - \omega^2\mathbf{M})\mathbf{\Phi} = 0. \tag{4.5}$$

This equation contains a trivial solution $\mathbf{\Phi} = 0$, implying a system with no motion. The equation contains non-trivial solutions if

$$\det(\mathbf{K} - \omega^2\mathbf{M}) = 0. \tag{4.6}$$

The solution gives an equal amount of solutions as the amount of dofs for the natural frequencies, also referred to as eigenfrequencies, ω_n. Each eigenfrequency provides a corresponding natural mode of vibration, or eigenmode, $\mathbf{\Phi}$, which can be determined from Equation 4.5. The eigenfrequencies and eigenmodes of the undamped system are natural properties of the system and depend on its mass and stiffness.

4.2.2 Steady-state dynamics

For an undamped sdof system subjected to a forced harmonic load, Equation 4.1 can be written as

$$m\ddot{u} + ku = p_o sin(\omega t), \tag{4.7}$$

where p_o is the magnitude of the force and ω is the forcing frequency. The response of a system subjected to this force will be a combination of a steady-state response and a transient response with the latter being dependant on the initial conditions of the system. For a damped system, the transient vibration will decay leaving only the steady-state vibration when the harmonic load is applied. The steady-state analysis can be expressed in terms of a complex-valued frequency-domain response. The complex load and displacement response can be written as:

$$\mathbf{p}(t) = \hat{\mathbf{p}} e^{i\omega t}, \tag{4.8}$$

$$\mathbf{u} = \hat{\mathbf{u}} e^{i\omega t}, \tag{4.9}$$

where $\hat{\mathbf{p}}$ is the complex load amplitude and $\hat{\mathbf{u}}$ is the complex displacement amplitude. Inserting these expressions into Equation 4.2 yields the following expression:

$$\mathbf{D}(\omega)\hat{\mathbf{u}} = \hat{\mathbf{p}}, \tag{4.10}$$

where $\mathbf{D}(\omega)$ is the dynamic stiffness matrix defined as

$$\mathbf{D}(\omega) = -\omega^2\mathbf{M} + i\omega\mathbf{C} + \mathbf{K}. \tag{4.11}$$

4.2.3 Resonance

Resonance is a phenomenon causing a system to vibrate at significantly higher amplitudes in certain frequencies, known as resonance frequencies or eigenfrequencies. The simplest way to describe resonance is by considering the undamped sdof version of Equation 4.7. This results in the expression

$$\hat{u} = \frac{\hat{p}}{-\omega^2 m + k}, \tag{4.12}$$

where $\hat{p}$ is assumed to be independent of frequency in this case. The natural frequency is defined as

$$\omega_n = \sqrt{\frac{k}{m}}, \tag{4.13}$$

and the static displacement is

$$u_{st} = \frac{\hat{p}}{k}. \tag{4.14}$$

A deformation factor for the dynamic response in relation to the static response can then be derived as:

$$\frac{\hat{u}}{u_{st}} = \frac{1}{1 - \left(\frac{\omega}{\omega_n}\right)^2}. \tag{4.15}$$

As the frequency of the harmonic force approaches the natural frequency of an undamped system, called the *resonant frequency*, the deformation factor approaches an infinite value as seen in Figure 4.1. In reality, damping is always present and the deformation factor for damped systems reach a finite maximum value at the resonant frequency.

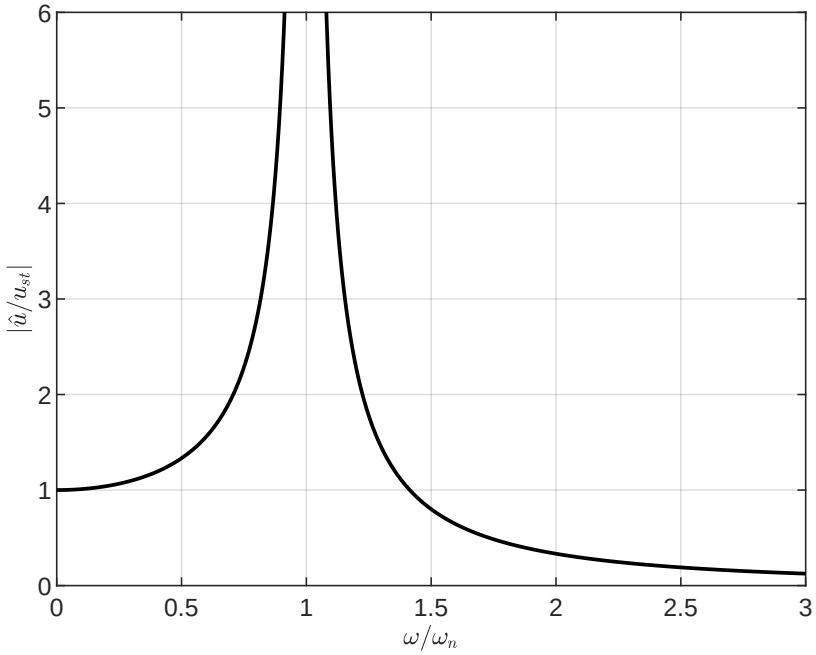

Figure 4.1: Deformation factor of an undamped system subjected to a harmonic load, as a function of the excitation frequency ω.

4.2.4 Damping

A vibrating system continuously dissipates energy through damping causing the amplitude to diminish during free vibration. Damping often occurs as a combination of multiple mechanisms, examples being friction between structural elements, or friction between material particles and fibres. A method to represent the damping of a system is by estimating the energy loss in a cycle of harmonic vibration. The energy dissipated by viscous damping in a cycle of harmonic vibration of the sdof system in Equation 4.1 is

$$E_D = \pi c \omega u_o^2, \tag{4.16}$$

while the maximum strain energy during a cycle is

$$E_{So} = k u_o^2 / 2. \tag{4.17}$$

The specific damping factor, or the *loss factor* is defined as

$$\eta = \frac{1}{2\pi} \frac{E_D}{E_{so}} = \frac{c\omega}{k}. \tag{4.18}$$

Substituting c in Equation 4.16 with the loss factor in Equation 4.18 gives the following expression:

$$E_D = \pi \eta k u_o^2. \tag{4.19}$$

This expression gives a rate-independent damping where the energy dissipation in a cycle is independent of the vibration frequency, ω.

4.3 Wave propagation

Wave propagation in soils can be divided into two types: body waves and surface waves. Body waves can in turn be divided into pressure waves (P-waves) and shear waves (S-waves). P-waves create compression and expansion of the soil, with particles moving parallel to the propagation direction. In S-waves, particles move in shearing, perpendicular to the propagation direction. Rayleigh surface waves travel close to the surface with particles moving through a combination of pressure and shearing. The particle motions of the different wave types are illustrated in Figure 4.2.

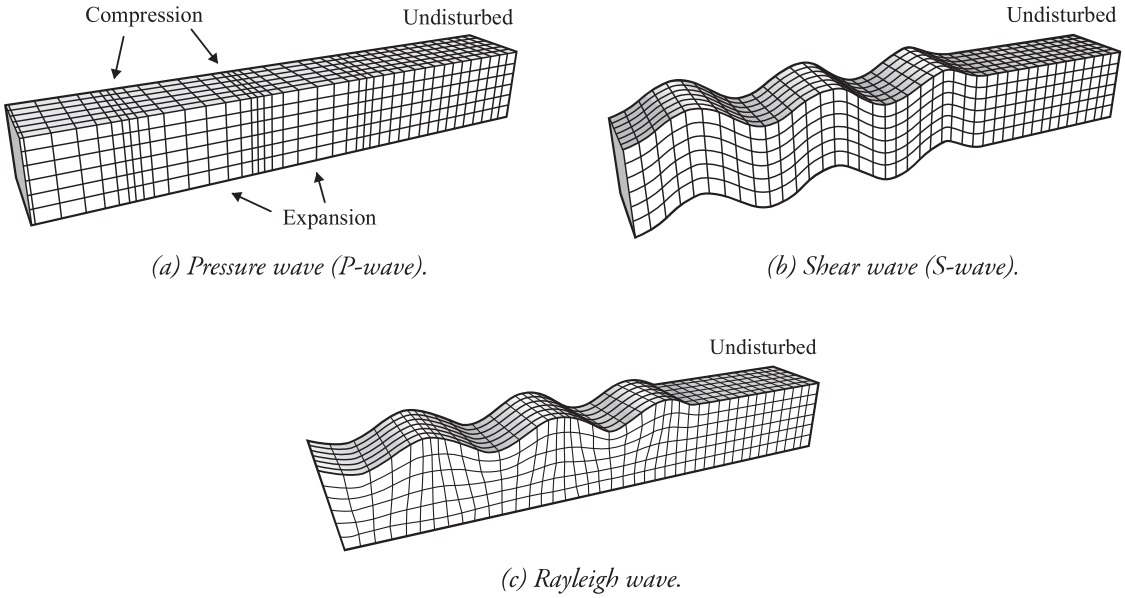

(a) Pressure wave (P-wave).

(b) Shear wave (S-wave).

(c) Rayleigh wave.

Figure 4.2: Propagation of wave types found in soil [17].

The propagation speed of P-waves and S-waves is given by

$$c_P = \sqrt{\frac{\lambda_L + 2\mu}{\rho}}; \quad c_S = \sqrt{\frac{\mu}{\rho}} \tag{4.20}$$

where ρ is the mass density, λ_L and μ are the first and second Lamé constants. The Lamé constants are material properties of the medium defined as

$$\lambda_L = \frac{vE}{(1+v)(1-2v)}; \quad \mu = \frac{E}{2(1+v)} \tag{4.21}$$

where E is the Young's modulus and v is Poisson's ratio.

4.4 Modelling of footsteps

A common source of vibrations and structure-borne sound are the impacts due to human walking. The human gait can be seen as periodic events of impulse loading

along an element as a time-varying load over the course of each footstep. The ground reaction force (GRF) from a footstep has been researched using measurements with humans walking on a force plate. The load pattern varies with the speed of walking, from slow walk to running and can for normal walking be divided into multiple stages. For normal walking, the first peak in GRF is the heelstrike of the foot followed by a second peak as the point of contact is moved towards the toe as can be seen in Figure 4.3a. The second peak is then followed by the heelstrike of the second foot represented by the dashed line in Figure 4.3a as the first foot is lifted off the ground creating an overlap between the impacts. The GRF is proportional to the body weight of the subject walking and is thus favourably presented as a percentage of the body weight. For normal walking, the time length of the contact is typically around 600 ms with the walking frequency roughly following a normal distribution as seen in figure 4.3b with a mean frequency of 2 Hz [30] and a standard deviation of 0.173.

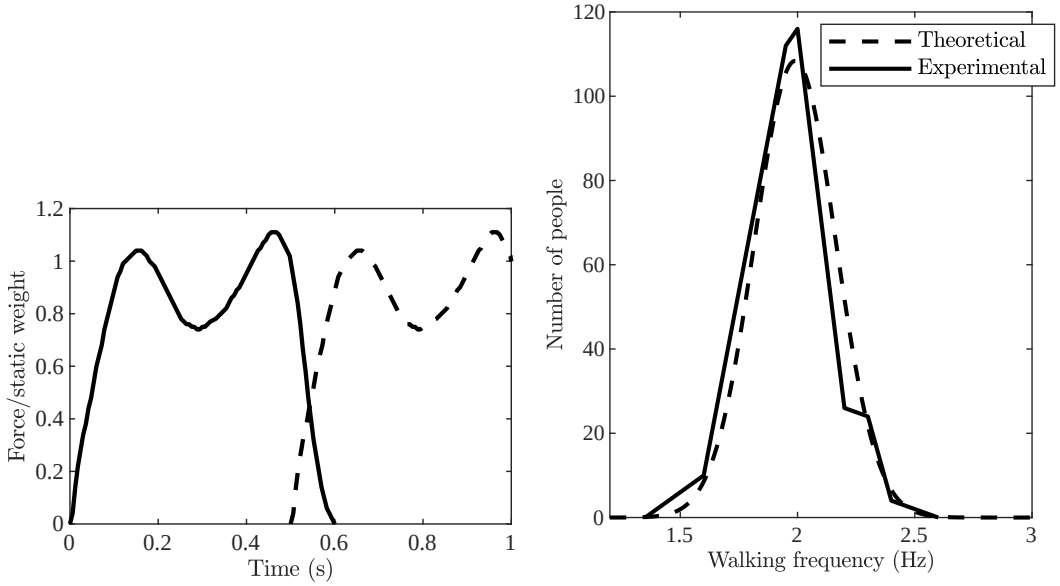

(a) Typical load pattern and GRF for normal walking

(b) Experimental walking frequencies and theoretical normal distribution

Figure 4.3: Load pattern and walking frequency for normal walking [30].

The force pattern is also dependent on what the subject is wearing as well as the type of surface. Typically, a harder surface will produce a higher force over a shorter period of time compared to a softer surface.

4.5 Evaluation metrics for vibration

In order to evaluate the vibrations, it is convenient to have comparative metrics linked to physical meanings. In this section, various methods for calculating the vibrational performance are presented.

4.5.1 Root mean square

When evaluating the vibrational response of a structure, RMS can be used. The RMS can be used to give a single scalar value of an FRF. The RMS of an FRF V(f) is calculated as:

$$V_{RMS} = \sqrt{\frac{1}{n}\sum_{i=1}^{n} V_i(f)^2} \tag{4.22}$$

where n is the number of studied frequencies and V_i is the value for the studied frequency.

4.5.2 Vibration dose value

The VDV is a parameter taking into account both the magnitude of the vibration and the time frame in which it occurs. The VDV uses a root-mean-quad of the acceleration time and gives a cumulative value on the vibration over a period of time. It is defined as

$$VDV = \left(\int_0^T a(t)^4\, dt\right)^{1/4} m/s^{1.75}. \tag{4.23}$$

An estimated vibration dose value (eVDV) can be calculated with the RMS acceleration and the cumulative exposure duration. For a crest factor below 6, defined as the ratio between the peak acceleration and the RMS, the eVDV is calculated as

$$eVDV = 1.4 a_{rms} t^{1/4}. \tag{4.24}$$

4.5.3 Equivalent radiated power

A method of estimating the radiated sound from a vibrating element is by the use of the equivalent radiated power (ERP). The ERP is a measure dependent on the velocity normal to the surface of a vibrating panel and is used to approximate the radiated sound power from an element across a fluid. The ERP is calculated as:

$$ERP = \frac{1}{2}\rho_f c_f \int_A |v_n|^2 dA, \tag{4.25}$$

where ρ_f is the density of the fluid, c_f is the speed of sound in the fluid, $|\mathbf{v_n}|$ is the velocity normal the radiating surface and A is the area of the radiating surface. For a finite element analysis, Equation 4.25 can be formulated as a sum of the radiated power from each element as:

$$ERP = \frac{1}{2}\rho_f c_f \sum_{i=1}^{N_e} A_e |v_n|^2 \tag{4.26}$$

where A_e is the area of each element, $|v_n|$ is the velocity of the node adjacent to the elements and N_e is the number of elements of the surface. The ERP is based on assumptions of inelasticity in the structure and plane waves in the acoustic medium which implies a perfect radiation. The ERP-level can be described using a logarithmic scale denoted in decibels (dB) as following:

$$L_{ERP} = 10log\left(\frac{ERP}{ERP_{Ref}}\right), \tag{4.27}$$

where ERP_{Ref} is a reference value set to 10^{-12} in this report.

In order to calculate the ERP over the whole area of the floor the velocities in the elements adjacent to each node is approximately considered to be equal to the velocity of the observed node. For a 4-node element this is done by applying a constant velocity to an area equal to the element area for a node adjacent to four elements. For nodes along the edge, only adjacent to two elements, the area is set to half the element area, and it is set to a quarter of the element for a node located in the corner.

5 Reference case 1: floor panel

In this chapter, LCA and dynamic analysis of a floor panel is presented. The analysis is conducted for a prestressed concrete floor panel of type RDF 240/20, a seven-layered CLT panel, and a composite floor panel consisting of concrete with a seven-layered CLT panel underneath. All floors panels have equal length and width. The layer thickness of the CLT floor panel is varied. The different floors are evaluated in terms of balance between the vibroacoustic properties and the environmental indicators EE and GWP. The prestressed concrete floor panel is used as a reference for the comparison with the other floor panel types.

The static design of the concrete floor panel is performed using span tables provided by the manufacturer in [31]. The CLT floor panel is designed according to guidance provided in [32] in accordance with eurocode 5. The characteristic load used in the design is set to 2.5 kN/m^2 representing a load in office areas. The concrete floor panel and the lowest thickness of the CLT are thus verified to fulfil the ultimate limit state and the serviceability limit state.

5.1 Floor panel dimensions

The floor panels in this reference case have the dimensions 2.4 m x 7.0 m (width x length). The CLT floor panels have varying thicknesses, t, of 30 mm–50 mm in each ply (210 mm–350 mm total thickness). The plies are orientated perpendicular to the plies in adjacent layers as shown in Figure 5.1. The CLT floor panel is composed of spruce plies with strength class C24.

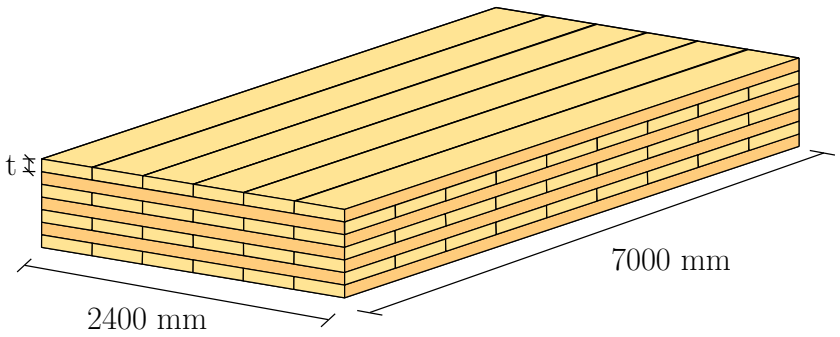

Figure 5.1: Visualisation of the CLT floor panel used in the reference case including ply orientation.

The composite floor panel consists of 80 mm concrete on top of a seven-layered CLT floor panel with a thickness of 35 mm in each ply (245 mm total thickness of the CLT floor panel). The concrete layer has the strength class C45, the CLT floor panel is composed of spruce plies with strength class C24.

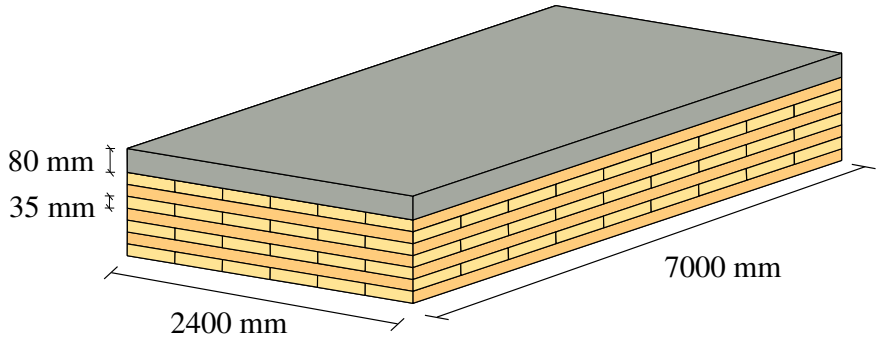

Figure 5.2: Visualisation of the composite floor panel used in the reference case.

The concrete floor panel is composed of a 200 mm prestressed concrete with the strength class C45. The reinforcement is considered in the LCA. In the dynamic analysis, a floor panel with homogeneous concrete is used, i.e. the reinforcement is neglected. The concrete floor panel is illustrated in Figure 5.3. Concrete floor panels with thicknesses 150 mm and 250 mm are also investigated for footstep loading.

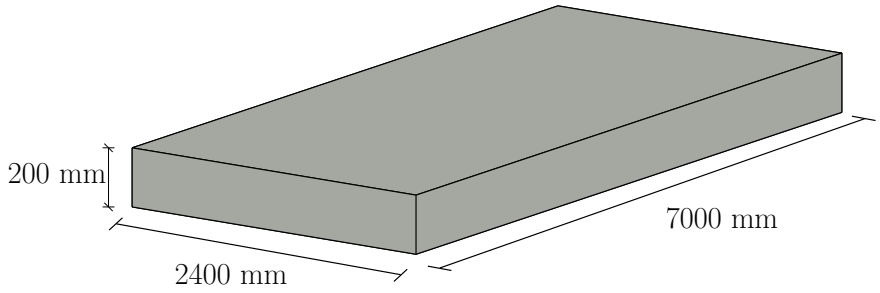

Figure 5.3: Visualisation of the concrete floor panel used as reference case.

5.2 LCA

The values calculated for GWP and EE, regarding modules A1–A3 for the concrete floor panel and the CLT floor panel, are based on EPDs conducted by The Norwegian EPD Foundation. The EPDs apply for a prestressed concrete floor panel produced by Strängbetong AB [33] and CLT produced by Martinssons Såg AB [34]. For the composite floor panel, the CLT floor panel is identical to the pure CLT floor panel, while the values used for the concrete layer used are from ÖKOBAUDAT [35]. ÖKOBAUDAT is a database created by the German Federal Ministry of the Interior, Building and Community containing LCA datasets from either specific products or German averages.

5.2.1 Transport to construction site

The module A4 consists of the transport to the construction site which depends on the location of the construction in relation to the factories. For instance, the production facility for the CLT manufactured by Martinsons is located in northern Sweden while

Strängbetong has facilities in multiple areas around Sweden. Due to this, a favour will be gained towards the choice of concrete if the construction site is located in the southern Sweden. As this case study does not have a specific location, a transport distance of 200km is chosen. This choice of distance makes the difference in weight between the different floor panels significant, while not being a dominating factor.

The parameters used for the calculations of the A4 module presented in Table 5.1 are from ÖKOBAUDAT. These calculations are based on a truck-trail transport using diesel as fuel following the European emission standard EURO 5. Reference unit for the calculations is 1000kg and km [t km].

Table 5.1: Reference values used for module A4 in the reference case.

Indicator	Unit/(t km)	A4
PERE	MJ	0.05164
PENRE	MJ	0.864
GWP	$kgCO_2 - e$	0.06444

5.2.2 Construction-installation process

The construction and installation process is considered in the A5 module of the LCA and consists of the impact and resource use during the on-site construction of the building. This includes the use of any machinery and equipment at the construction site and is something that varies on a case basis. A difference depending on the construction material is expected and thus average values based on ÖKOBAUDAT are used in this analysis. The reference values for the A5 module are presented in Table 5.2.

Table 5.2: Reference values used for concrete and CLT for module A5 in the reference case.

Material	Indicator	Unit/m^3	A5
Concrete	PERE	MJ	5.89
	PENRE	MJ	13.66
	GWP	$kgCO_2 - eq$	1.08
CLT	PERE	MJ	0.053
	PENRE	MJ	0.284
	GWP	$kgCO_2 - eq$	1.768

5.2.3 Concrete floor panel

The concrete floor panel consists of 1.23 weight-% of steel reinforcement. Volumes and weight used in these calculations are 3.36 m^3, and 8064 kg respectively using a density of 2400 kg/m^3. Presented in Table 5.3 are the reference values per tonne (t) for modules A1–A3 according to the EPD for prestressed concrete [33]. Presented in Table 5.4 is the primary energy use and GWP for the concrete floor panel. For modules A4–A5 the reference values presented in Table 5.1 and Table 5.2 are used.

Table 5.3: Reference primary energy and GWP for prestressed concrete.

Indicator	Unit/t	A1–A3
PERE	MJ	259
PENRE	MJ	984
GWP	$kgCO_2 - eq$	159

Table 5.4: Primary energy and GWP for the 200 mm concrete floor panel.

Indicator	Unit	A1–A3	A4	A5	Total
PERE	MJ	2097	83	19.8	2200
PENRE	MJ	8064	1393	45.9	9503
Total energy	MJ	10161	1476	65.7	11703
GWP	$kgCO_2 - eq$	1282	104	3.6	1390

5.2.4 CLT floor panel

Volume and mass of the CLT floor panels are presented in Table 5.5 and are based on timber with a density of 430 kg/m^3. Reference values for modules A1–A3 are presented in Table 5.6 with values according to the EPD for CLT [34]. Modules A4–A5 are calculated according to the reference values in Table 5.1 and 5.2.

Table 5.5: Volume and mass of the studied CLT floor panels.

Ply thickness [mm]	Volume [m^3]	Mass [kg]
30	3.528	1517
35	4.116	1770
40	4.704	2023
45	5.292	2276
50	5.88	2528

Table 5.6: Reference values used for modules A1–A3 for CLT in the reference case.

Parameter	Unit/m^3	A1–A3
PERE	MJ	1595
PENRE	MJ	509
GWP	$kgCO_2 - e$	45.6

As timber products contain biogenic carbon dioxide, which during its end of life can be released with the energy as raw material recovered, these values are excluded in the analysis. The exclusion of these values implies that only the EE and GWP from the manufacturing and assembly stages is considered for the comparison, disregarding the end of life use of the wood. In Table 5.6 the reference values from the EPD is presented. Presented in Table 5.7, and Table 5.8 are the values for primary energy use, and GWP respectively.

Table 5.7: Primary energy use when varying the thickness of the CLT floor panel.

Thickness	Indicator [MJ]	Module			
		A1-A3	A4	A5	Total
30	PERE	5627	16	0.19	5643
	PENRE	1796	262	1	2059
	Total	7423	278	1.19	7702
35	PERE	6565	18	0.22	6583
	PENRE	2095	306	1.2	2402
	Total	8660	324	1.42	8985
40	PERE	7503	21	0.25	7524
	PENRE	2394	350	1.3	2745
	Total	9897	371	1.6	10270
45	PERE	8441	24	0.28	8465
	PENRE	2694	393	1.5	3089
	Total	11135	417	1.8	11554
50	PERE	9379	26	0.31	9405
	PENRE	2993	437	1.7	3432
	Total	12732	463	2	13197

Table 5.8: GWP when varying the thickness of the CLT floor panel.

Thickness	GWP [kg $CO_2 - eq$]			
	A1-A3	A4	A5	Total
30	160	20	6	186
35	188	23	7	218
40	215	26	8	249
45	241	29	9	279
50	268	33	10	311

5.2.5 Composite floor panel

Presented in Table 5.9 are the volume and mass for the composite floor panel, based on a concrete density of 2400 kg/m^3 and timber density of 430 kg/m^3.

Table 5.9: Volume and mass used for the composite floor panel in the reference case.

Part	Volume [m^3]	Mass [kg]
Concrete	1.344	3226
CLT	4.116	1770
Total	5.46	4996

The CLT floor panel used in the composite floor panel has equal primary energy and GWP to the 35 mm ply thickness CLT floor panel presented in Table 5.7 and Table 5.8. The concrete layer is not reinforced and values for C45 concrete from ÖKOBAUDAT are used; these are presented in Table 5.10. Presented in Table 5.11 are the values for primary energy and GWP of the composite floor panel.

Table 5.10: Reference values from ÖKOBAUDAT for C45 concrete.

Indicator	Unit/m^3	A1–A3
PERE	MJ	282
PENRE	MJ	1500
GWP	$kgCO_2 - eq$	286

Table 5.11: Primary energy and GWP for the composite floor panel.

Indicator	Unit	Module			
		A1–A3	A4	A5	Total
PERE	MJ	6944	52	8	7004
PENRE	MJ	4111	863	20	4994
Total energy	MJ	11055	915	28	11998
GWP	$kgCO_2 - eq$	572	64	8	644

5.2.6 Summary of LCA

Presented in Figure 5.4 is the primary energy use for the investigated floor panel types. It is seen that the concrete floor panel has a significantly higher non renewable energy use compared to the other floor panels. The total energy use for the CLT floor panel with ply thickness 50 mm and the composite floor panel is higher compared to the concrete floor panel.

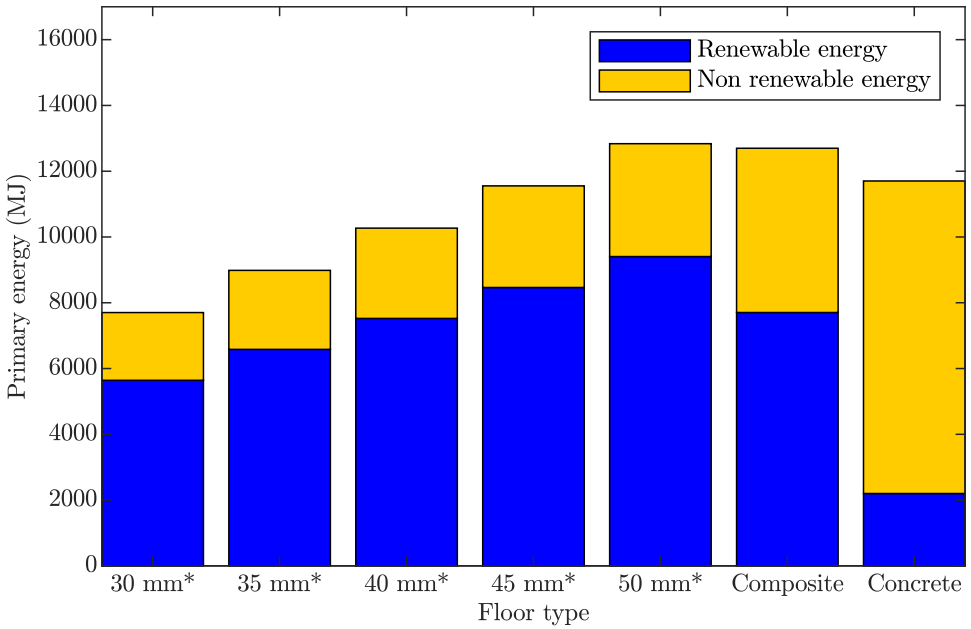

Figure 5.4: Primary energy use for the investigated floor panels. *Ply thickness of the CLT floor panel.

Presented in Figure 5.5 is the GWP of the investigated floor panels. It is seen that the CLT floor panels have a significantly lower GWP compared with the other floor panels. For the composite floor panel, the GWP is approximately half compared with the concrete floor panel, but over twice as high compared with the 50 mm CLT floor panel.

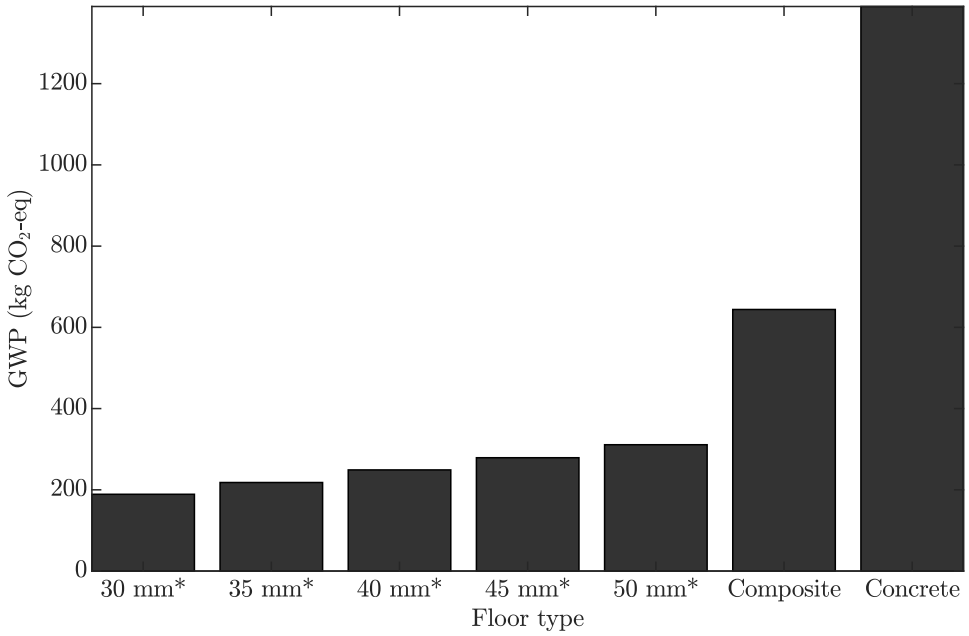

Figure 5.5: GWP of the investigated floor panels. *Ply thickness of CLT floor panel.

5.3 Numerical model

The floor panel is simply supported continuously along the short edges with the boundary conditions placed in the middle of the cross-section in the transverse direction. Placement of the load is set at point P1 as shown in Figure 5.6 in order to excite many modes within the observed frequency range. Evaluation of the vibration is done on either all FE mesh nodes of the floor panel or in one mesh node located at P2. The numerical model is meshed using 4-node linear shell elements (S4R) in Abaqus.

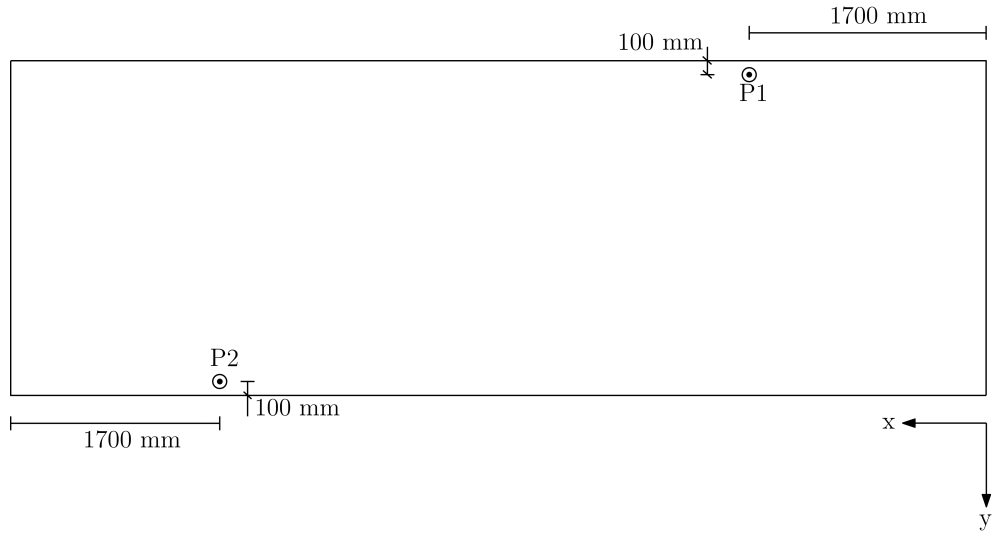

Figure 5.6: Load placement (P1) and evaluation point (P2).

The CLT floor panel is modelled as C24 spruce with the material properties according to Table 5.12a. Young's modulus and Poisson's ratio are defined in the longitudinal (L), radial (R) and tangential (T) directions, where the radial direction is assumed to be aligned with the thickness direction of the panel. The plies of the CLT floor panel are modelled using a seven-layered composite layup with each layer oriented as shown in Figure 5.1 assuming full interaction between the plies and layers. The concrete floor panel is modelled as a homogeneous shell section with material properties of C45 concrete according Table 5.12b. The FE mesh used is shown in Figure 5.7 with the element size 0.1 m x 0.1 m in order to achieve a minimum of 6 nodes for a whole wavelength at the highest frequency considered.

Table 5.12: Material parameters used for the floor panels.

(a) Material properties for the timber.

Material	C24 Timber
Density(kg/m^3)	430
E_L (MPa)	11000
E_R (MPa)	370
E_T (MPa)	370
G_{LR} (MPa)	590
G_{LT} (MPa)	590
G_{RT} (MPa)	23
v_{LR} (-)	0.38
v_{LT} (-)	0.51
v_{TR} (-)	0.31
$Loss\ factor$ (-)	0.06

(b) Material properties C45 concrete.

Material	Concrete C45
Density (kg/m^3)	2400
E (MPa)	36000
v (-)	0.2
$Loss\ factor$ (-)	0.03

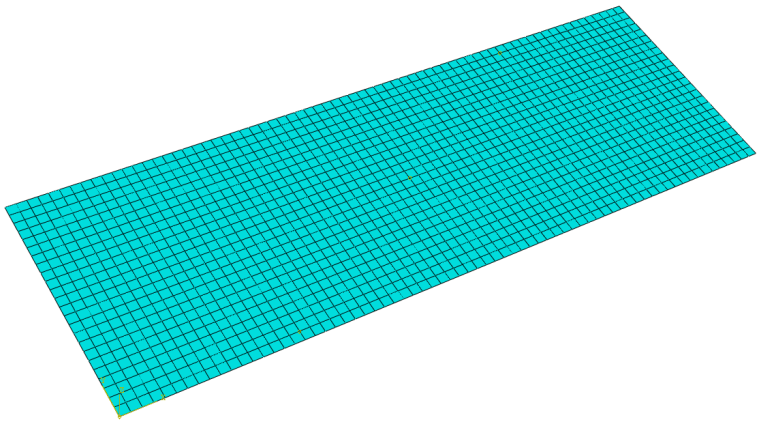

Figure 5.7: Visualisation of the FE mesh used for all floor panels.

For ERP calculations, all FE elements were evaluated. The density, ρ_f and the speed of sound c_f are presented in Table 5.13.

Table 5.13: Density and speed of sound in air used for the ERP calculation.

Parameter	Value
ρ_f (kg/m^3)	1.22
c_f (m/s)	340

5.3.1 Footstep loading

The evaluation of the vibration due to footstep is done by performing a transient analysis using modal dynamics with a time step of 1 ms. The modelling of the footstep is done by creating a time-varying load representing a 70kg subject walking barefoot. The load pulse used for this analysis is shown in Figure 5.8.

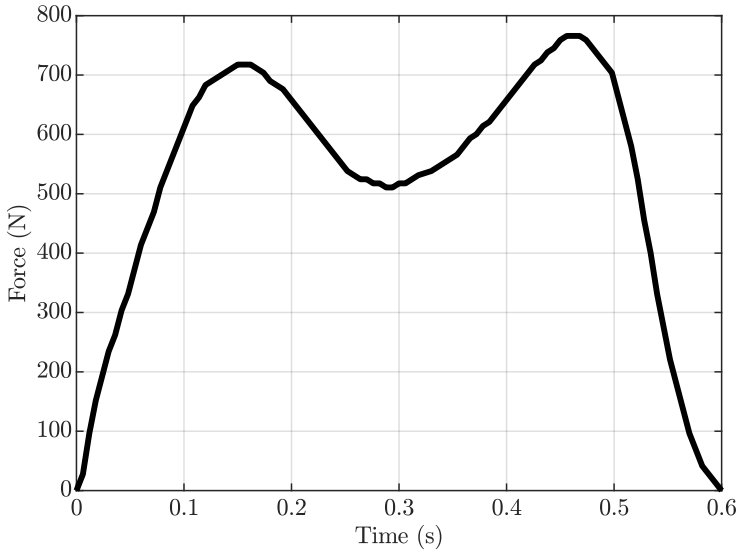

Figure 5.8: Load pattern for a footstep used in the analysis

To model the effect of multiple footsteps through walking, the response from one step is overlapped during post-processing with the frequencies 2 Hz, 1.83 Hz and 2.16 Hz, these frequencies being the mean rate according to [30], and one standard deviation lower, and higher respectively. This does not model the effect of a subject walking across the floor panel but rather a subject stepping on the exact same spot at a constant rate.

5.4 Parameter study

The LCA and the vibration response of the CLT floor panel and the composite floor panel as a function of the ply thickness is investigated using the 200 mm thick concrete floor panel as a reference. The vibration analyses are performed for a unit point load using steady state direct analysis and for a footstep load using modal transient analysis. Scalar values of the vibration response in relation to EE and GWP is investigated as the ply thickness varies. The frequency range considered is between 1 Hz–178 Hz with the higher frequency being the upper limit in the 160 Hz 1/3 octave band.

5.4.1 Steady-state analysis with unit point load

Presented in this section are the frequency responses for the steady state analysis with a unit point load in P1. Figure 5.9 shows the complex magnitude of the velocity frequency response between frequencies 2 Hz–80 Hz in point P2. A scalar value, representing the RMS of the velocity FRF between 1 Hz–80 Hz is calculated. The RMS velocities of the floor panels are divided by the RMS velocity of the 200 mm thick concrete floor panel in order to present the velocity of the different floor panels in relation to the concrete floor panel. The concrete floor panel has, within the considered frequency range, fewer resonance peaks and a significantly lower amplitude of the peaks. For the CLT floor panel, it is seen that an increased thickness reduces the

amplitude of the response and shifts the resonance peaks to a higher frequency.

The relative RMS velocity is then compared with the relative environmental impact, calculated as the total energy, non-renewable energy and GWP of the investigated floor panels, divided by the corresponding values for the concrete floor panel and is presented in Figure 5.10. The same relative environmental impact is applied in all figures describing the balancing hereafter. It is seen that no investigated floor panel has a lower RMS velocity compared with the 200 mm thick concrete floor panel, with the composite floor panel having a lower RMS velocity in relation to the pure CLT floor panels. Increasing the thickness of the CLT floor panel reduces the RMS velocity. The composite floor panel, and the 50 mm ply thickness CLT floor panel surpass the total energy consumption of the concrete floor panel, while the non-renewable energy consumption and GWP of all floor panels is significantly lower than the concrete floor panel.

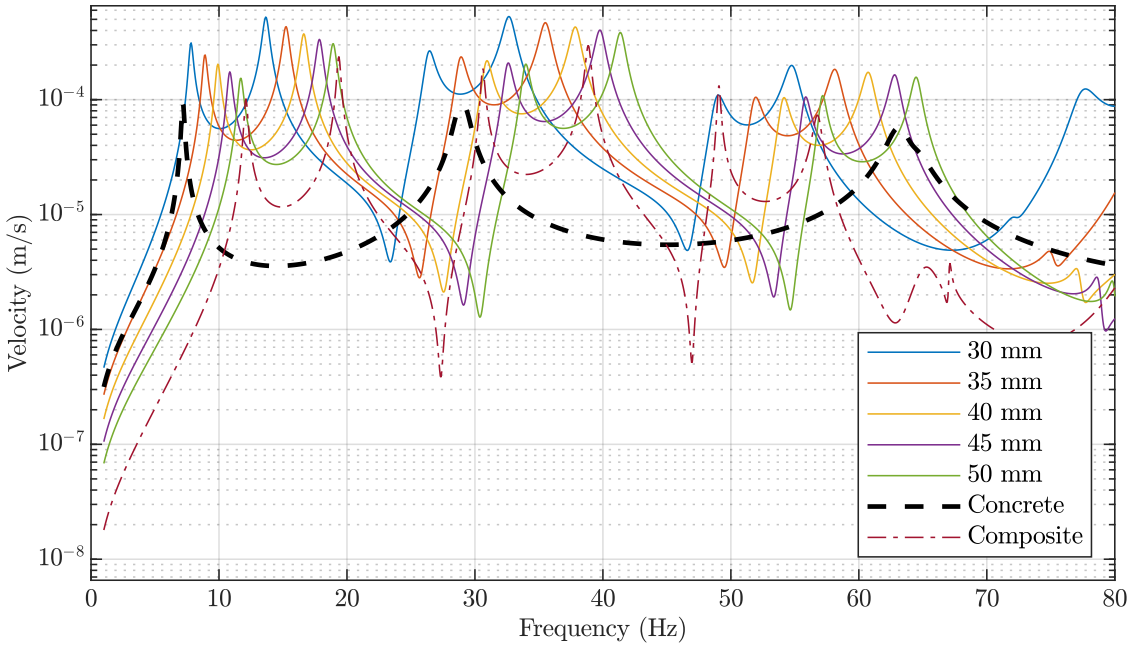

Figure 5.9: Velocities at point P2 for the different floor panels.

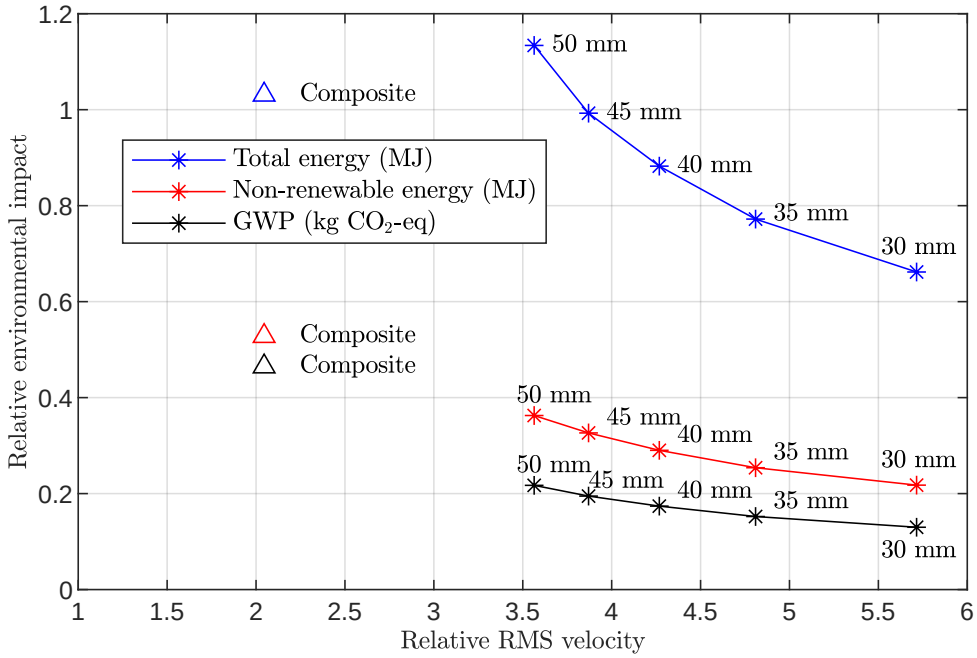

Figure 5.10: Environmental impact and RMS velocity for the CLT floor panel and the composite floor panel relative to the 200 mm concrete floor panel at frequency range 1 Hz–80 Hz.

The ERPs of the whole floor panel surface are presented in Figure 5.11 for all investigated floor panels. A scalar value representing the RMS of the ERP is calculated between 20 Hz–178 Hz for all floor panels and divided by the ERP RMS of the 200 mm thick concrete floor panel. The relative ERP RMS and the relative environmental impact is presented in Figure 5.12. It is seen that the RMS of the ERP is higher for all floor panels in relation to the 200 mm thick concrete floor panel. The RMS of the ERP for the composite floor panel is higher than the pure CLT floor panels with a ply thickness of 35 mm and above due to the large peaks in the higher frequency range. A diminishing decrease in the ERP is seen as the ply thickness of the CLT floor panels is increased past 40 mm.

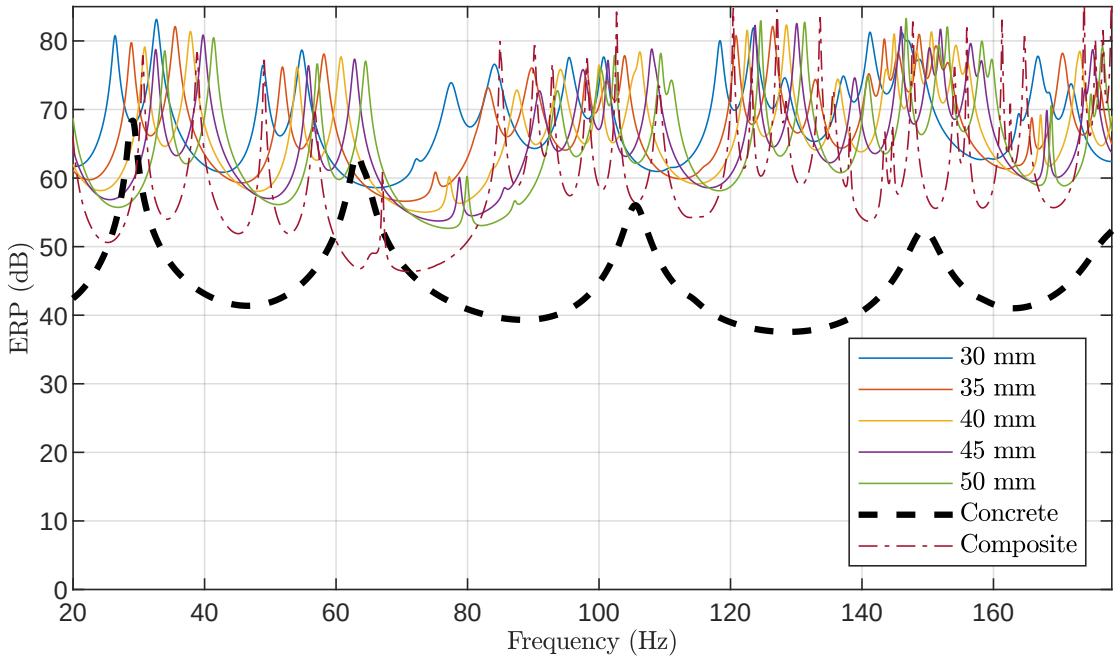

Figure 5.11: ERP for the different floor panels.

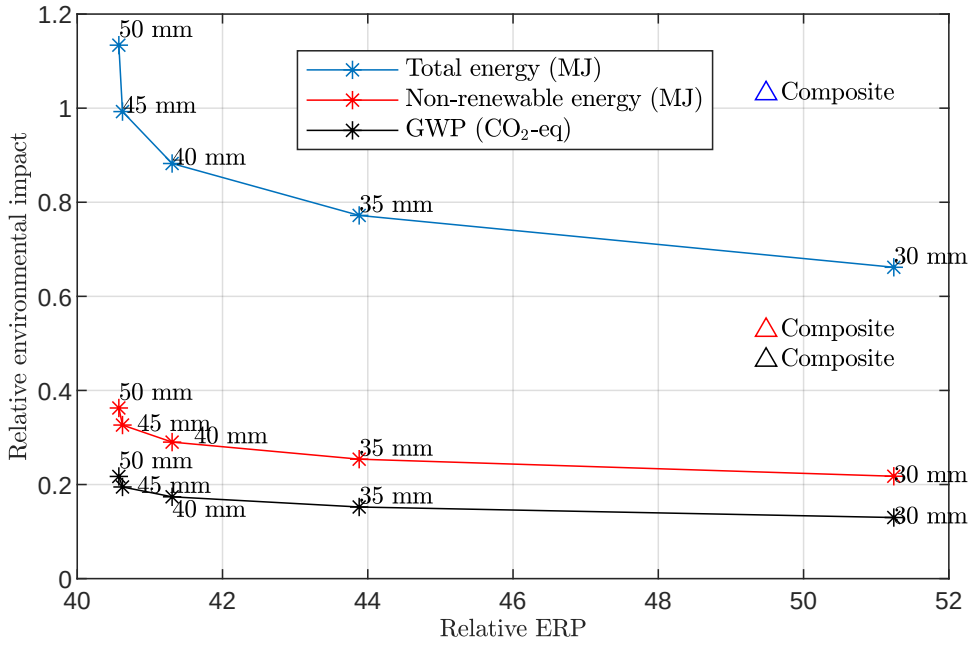

Figure 5.12: Environmental impact and ERP for the CLT floor panel and the composite floor panel relative to 200 mm concrete floor panel at frequency range 20 Hz–178 Hz.

5.4.2 Transient analysis of footstep pulse

Figure 5.13 shows and example of an acceleration response, namely the concrete floor panel with the responses of a single footstep overlapped at the rate of 2 Hz. The

post-processing of results is performed for the 0.5 s time period, highlighted in red in Figure 5.13, where the steady-state response has been reached.

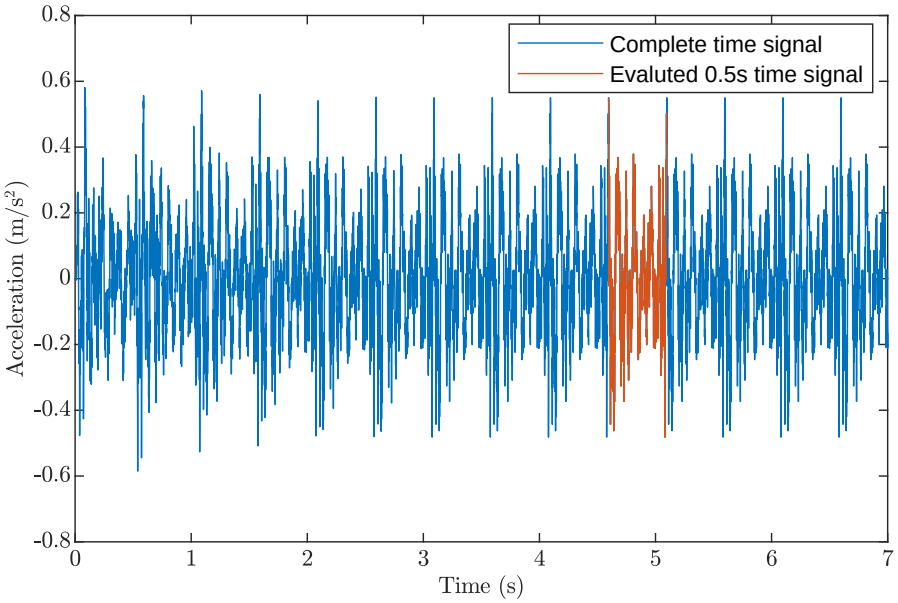

Figure 5.13: Acceleration time signal of the concrete floor panel for a walking frequency of 2 Hz. Time-window of 0.5 s used for evaluations is shown in red.

Balancing using weighted acceleration levels at point P2

Presented in Figure 5.14 are the frequency spectra for the different floor panels evaluated at P2 for a walking rate of 2 Hz (frequency spectra for walking frequencies 1.83 Hz and 2.17 Hz are presented in Appendix A). The frequency spectra are obtained by performing an FFT, with the weighting spectrum shown in Section 3.2.2 applied. For the walking frequency 2 Hz, it can be seen that the CLT floor panel with ply thickness 40 mm has a higher RMS value compared with the CLT floor panel with 35 mm thickness. For both the 1.83 Hz and 2.17 Hz walking frequencies it is seen that the CLT floor panel with 45 mm ply thickness has a higher RMS acceleration compared with the 40 mm ply thickness floor panel. Consequently, the frequency content of the footstep loading results in thicker floor panels sometimes being worse in terms of vibration amplitude.

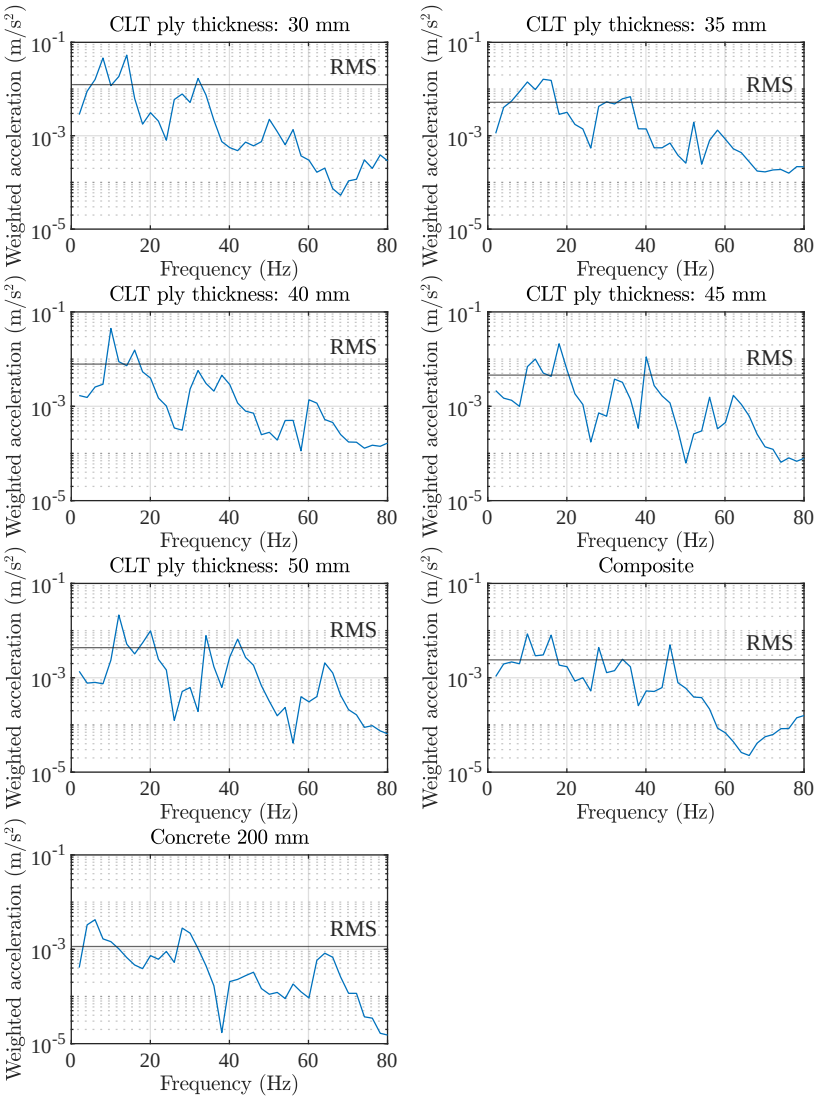

Figure 5.14: Frequency spectra of the weighted accelerations due to footsteps at a walking rate of 2 Hz for the different floor panels as evaluated at P2.

The relative weighted RMS acceleration presented in Figure 5.15 is obtained by first calculating a linear average between the acceleration spectra for the three different walking frequencies. Second, the RMS of the average frequency spectrum is calculated for each floor panel. The RMS values of the composite floor panel, the CLT floor panel, the 150 mm concrete floor panel, and the 250 mm concrete floor panel are divided with the RMS value for the 200 mm concrete floor panel to obtain the relative weighted RMS acceleration. For the 150 mm and 250 mm concrete floor panels, all environmental impact parameters scale equally in relation to the reference 200 mm concrete floor panel, therefore only one point is seen. To establish the relative environmental impact, the renewable energy, non renewable energy and GWP of the different floor panels are divided with corresponding values for the 200 mm thick concrete floor panel. It is seen that the relative RMS acceleration decreases with a greater ply thickness for the CLT floor panel. The composite floor panel results in roughly 1.3 times the weighted RMS acceleration compared with the concrete floor panel; a clear improvement compared to the thickest CLT floor panel which results in a factor 2.3. Increasing the thickness

of the concrete floor panel to 250 mm decreased the weighted RMS acceleration by 72%, while decreasing the thickness of the concrete floor panel to 150 mm increased the weighted RMS acceleration by 142% resulting in a similar value to the 50 mm ply thickness CLT floor panel.

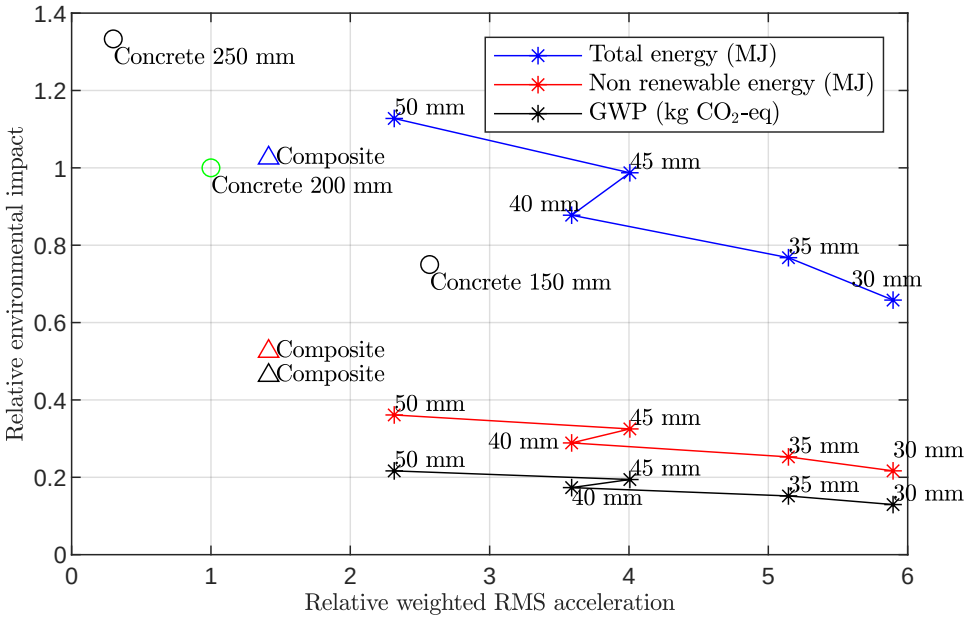

Figure 5.15: Environmental impact vs weighted RMS acceleration due to footsteps for the investigated floor panels, relative to the 200 mm thick concrete floor panel considering frequencies 1 Hz–80 Hz.

Balancing using base curve in ISO 10137

Using the base curve provided in ISO 10137 provides a metric for evaluation with reference to vibration levels where humans are negatively affected by whole-body vibration. A comparison of the acceleration spectra for footstep loading with the base curve adjusted for office areas according to ISO 10137 is shown in Figure 5.16 for the different floor panel types. It is seen that only the CLT floor panel with ply thickness between 30 mm–45 mm exceed the base curve values, between the frequencies 5 Hz–16 Hz.

The RSS of the base curve exceedance in the 1/3 octaves band is presented in Figure 5.17 along with the environmental impact in relation to the concrete floor panel. A similar result is seen as in Figure 5.15 where the 45 mm CLT floor panel has a higher exceedance of the base curve compared to the 40 mm CLT floor panel. The 50 mm CLT floor panel, the composite floor panel, the 250 mm thick concrete floor panel, and the 200 mm thick concrete floor panel has no exceedance of the base curve.

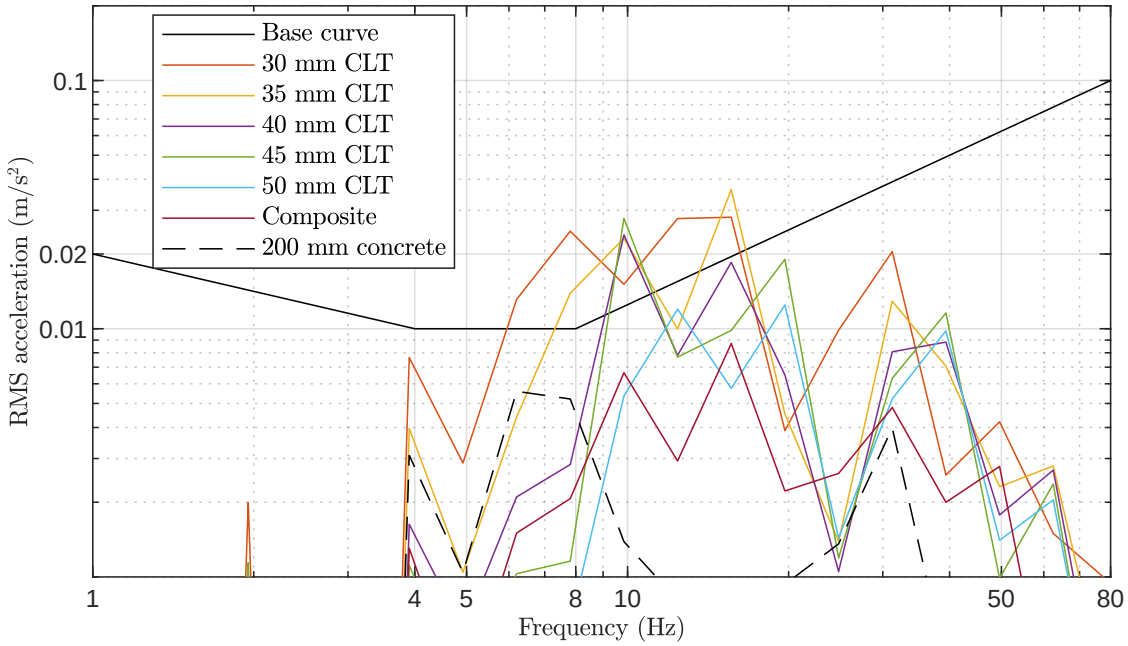

Figure 5.16: Base curve with weighted RMS acceleration spectra for the different floor panels.

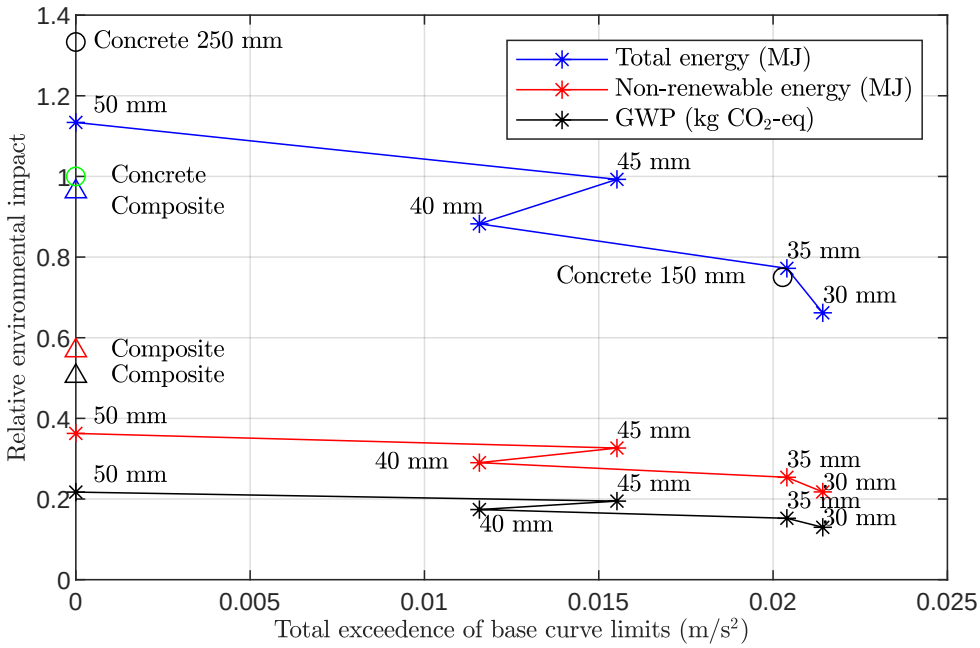

Figure 5.17: Total exceedance of the base curve (as shown in Figure 5.16) and the environmental impact of the CLT floor panels and composite floor panel relative to the 200 mm concrete floor panel.

Balancing using VDV

Using VDV as a metric provides a more appropriate method of evaluation to the base curve when the ratio between the peak value and the RMS value is greater than 6. VDV uses a root-mean-quad and provides a cumulative value over a long period

of time (8 h or 16 h in ISO 10137), rather than a mean over a short time period. Provided in Table 5.14 is the VDV of a single footstep cycle during the time period 0.5 s of the weighted acceleration time signal. Figure 5.18 shows a comparison of the environmental impact and VDV for the CLT floor panels in relation to the concrete floor panel. A similar result of the relative VDV can be seen as in the relative weighted acceleration presented in Figure 5.15. The highest performance of the timber floor panels is found in the composite floor panel with the VDV having a factor of 1.3 in relation to the 200 mm thick concrete floor panel. The highest performance of all floor panels is found in the 250 mm thick concrete floor panel with a factor of 0.4 in relation to the 200 mm concrete floor panel.

Table 5.14: Weighted average VDV of the different floor panels

floor panel	VDV ($m/s^{1.75}$)
30 mm	0.0471
35 mm	0.0406
40 mm	0.0271
45 mm	0.0317
50 mm	0.0185
Composite	0.114
Concrete	0.0084

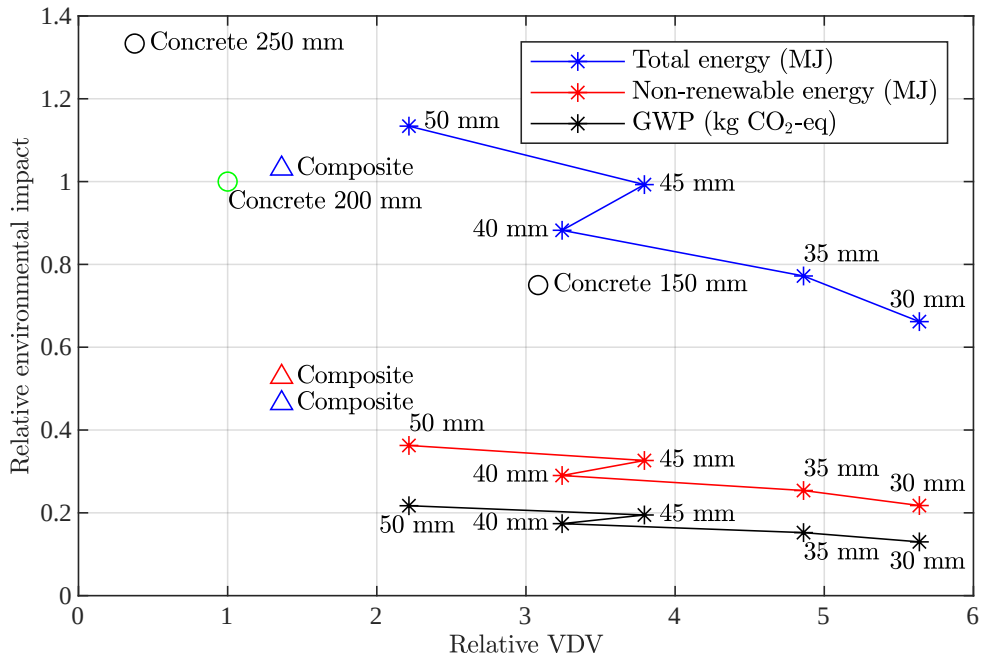

Figure 5.18: Weighted VDV of the CLT and composite floor panels in relation to the 200 mm thick concrete floor panel.

6 Reference case 2: building exposed to external loading

In this chapter, LCA and dynamic analysis of a building exposed to an external ground load is presented. A lightweight building consisting of floors of either CLT with varying ply thickness or CLT-concrete composite is investigated. The lightweight building is compared with a concrete building of equal dimensions where the balancing between the environmental impact and vibration is investigated.

6.1 Building and ground

The buildings have the dimensions 7 m x 2.4 m x 9 m (length x width x height) with three storeys consisting of a concrete foundation and three slabs (top slab being a roof) connected to columns separating the floor panels.

The analysis is performed for a lightweight building with glued laminated timber (glulam) columns, seven-layered CLT floor panels with ply thicknesses varying between 30 mm–50 mm, a concrete foundation and a seven-layered CLT roof with a ply thickness of 30 mm. The lightweight building is compared to a reference concrete building with the columns made of reinforced concrete and the floor panel and roof consisting of prestressed concrete. The building has been statically designed according to load case STR B 6.10b for an office building located in Lund using the values presented in Table 6.1.

Table 6.1: Characteristic snow load (s_k), characteristic load (q_k), reference wind velocity (v_b) and terrain type.

Parameter	Value
s_k(kN/m^2)	1.5
q_k (kN/m^2)	2.5
v_b (m/s)	26
Terrain type	III

The concrete building consists of reinforced concrete columns with strength class C45 and prestressed concrete floor panels with strength class C45. The lightweight building consists of glulam spruce columns with strength class C24, and floor panels and roof of the same type as presented in Chapter 5. Both buildings have concrete foundations with strength class C30. A visualisation of the buildings with the materials used is presented in Figure 6.1.

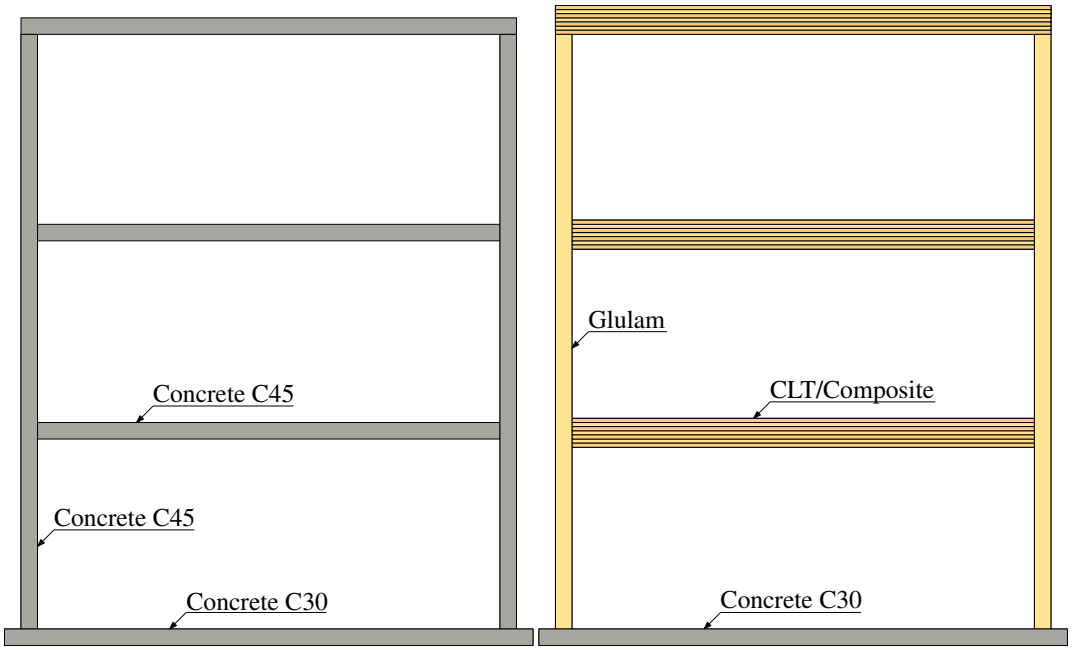

(a) Visualisation of the concrete building. **(b)** Visualisation of the timber building.

Figure 6.1: Illustration of the reference concrete building (a) and the lightweight building (b) with the materials used.

The ground consists of a surface layer of soil with a depth of 20 m. The response is investigated for either a soft, or a stiff soil. Underneath the soil is a 40 m layer of bedrock with a high density and stiffness in relation to the soil. As shown by the dashed lines in the illustration of the ground presented Figure 6.2, the ground in reality extends further in width and depth than what is modelled in this reference case.

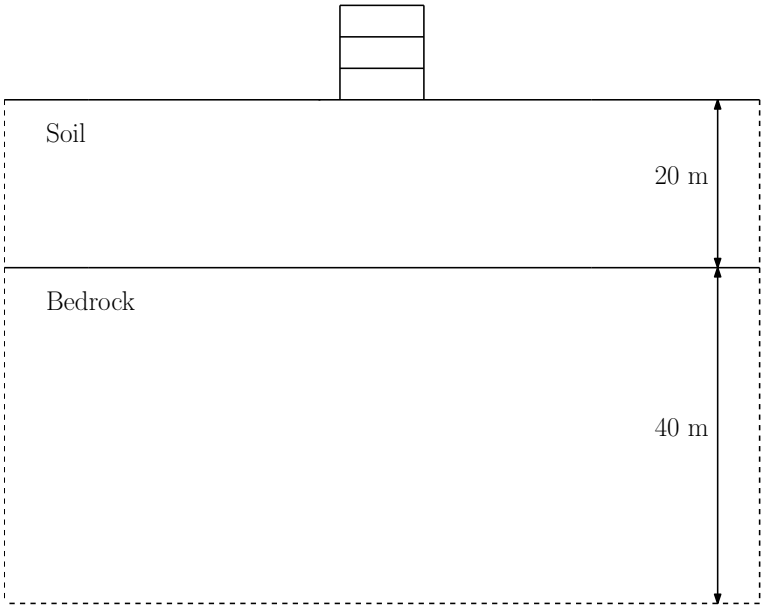

Figure 6.2: Illustration of the ground with depth of the different layers.

6.2 LCA

Presented in this section is the LCA for the different building elements in module A. The values are obtained from either EPDs or ÖKOBAUDAT. Reference values for module A4 are obtained from ÖKOBAUDAT with a transport distance of 200 km (see Section 5.2.1 for values).

6.2.1 floor panel

The building has two floor panels with either CLT with varying thickness, CLT-concrete composite, or prestressed concrete. As the material of the floor panels, together with the dimensions are the same as in Chapter 5, the values are identical for each floor panel. In Table 6.2 the primary energy use and GWP for module A1–A5 is presented for the different floor panels.

Table 6.2: Primary energy and GWP for the different floor panels.

floor panel	Indicator	Total
CLT 30mm	PERE (MJ)	11286
	PENRE (MJ)	4118
	Total energy (MJ)	15404
	GWP ($kgCO_2$-eq)	372
CLT 35 mm	PERE (MJ)	13166
	PENRE (MJ)	4804
	Total energy (MJ)	17970
	GWP ($kgCO_2$-eq)	436
CLT 40 mm	PERE (MJ)	15048
	PENRE (MJ)	5490
	Total energy (MJ)	20538
	GWP ($kgCO_2$-eq)	498
CLT 45 mm	PERE (MJ)	16930
	PENRE (MJ)	6178
	Total energy (MJ)	23108
	GWP ($kgCO_2$-eq)	558
CLT 50 mm	PERE (MJ)	18810
	PENRE (MJ)	6864
	Total energy (MJ)	25674
	GWP ($kgCO_2$-eq)	622
Composite	PERE (MJ)	14008
	PENRE (MJ)	9988
	Total energy (MJ)	23996
	GWP ($kgCO_2$-eq)	1288
Concrete	PERE (MJ)	4400
	PENRE (MJ)	19006
	Total energy (MJ)	23406
	GWP ($kgCO_2$-eq)	2780

6.2.2 Roof

The roof in the lightweight building is a seven-layered CLT panel with a thickness of 30 mm in each ply. The concrete building has a roof of the same type as the prestressed concrete floor panel. In Table 6.3, primary energy and GWP for module A1–A5 is presented using the reference values for the floor panels in Section 5.2.

Table 6.3: Primary energy and GWP for the roof.

Material	Indicator	A1-A3	A4	A5	Total
CLT	PERE (MJ)	5949	17	1	5967
	PENRE (MJ)	1898	277	6	2181
	Total energy (MJ)	7847	294	7	8148
	GWP ($kgCO_2$-eq)	171	21	2	192
Concrete	PERE (MJ)	2318	92	5	2415
	PENRE (MJ)	8808	1547	23	10378
	Total energy (MJ)	11126	1639	28	12793
	GWP ($kgCO_2$-eq)	1423	115	7	1538

6.2.3 Column

The columns in this analysis consist of either glulam or reinforced concrete. For the glulam, the reference values are based on the EPD for glulam manufactured by Martinsons AB [36]. The values from concrete are based on the EPD for concrete column manufactured by Strängbetong AB [37]. The reference values are presented in Table 6.4. Reference values for module A4 are from Section 5.2.1. Following that the building consists of 4 columns, the primary energy and GWP presented in Table 6.5 are based on the volume 1.44 m^3 and the weights 3456 kg for concrete, and 674 kg for glulam.

Table 6.4: Reference values for the columns used.

Material	Indicator/m^3	A1-A3	A5
Glulam	PERE (MJ)	11493	609
	PENRE (MJ)	527	108
	GWP ($kgCO_2$-eq)	33	3.2
Concrete	PERE	377	4
	PENRE (MJ)	1156	14
	GWP ($kgCO_2$-eq)	208	0.5

Table 6.5: Primary energy and GWP for the columns.

Material	Indicator	A1-A3	A4	A5	Total
Glulam	PERE (MJ)	16550	7	759	17316
	PENRE (MJ)	759	116	156	1031
	Total energy (MJ)	17309	123	915	18347
	GWP ($kgCO_2$-eq)	48	9	4.6	62
Concrete	PERE (MJ)	543	36	6	585
	PENRE (MJ)	1665	600	48	2313
	Total energy (MJ)	2208	636	54	2898
	GWP ($kgCO_2$-eq)	300	45	1	346

6.2.4 Foundation

The foundation used for both structures consists of C30 concrete with the dimensions 7.8 m x 2.4 m x 0.2 m (length x width x thickness). Reference values presented in Table 6.6 are for C30 concrete in ÖKOBAUDAT. Reference values for module A4 are from Section 5.2.1. Presented in Table 6.7 is the primary energy and GWP for the foundation.

Table 6.6: Reference values for the concrete foundation.

Indicator/m^3	A1-A3	A5
PERE (MJ)	204	6
PENRE (MJ)	1100	14
GWP ($kgCO_2$-eq)	219	1.08

Table 6.7: Primary energy and GWP for the foundation.

Indicator	A1-A3	A4	A5	Total
PERE (MJ)	763	39	22	824
PENRE (MJ)	4114	646	52	4812
Total energy (MJ)	4877	685	74	5636
GWP ($kgCO_2$-eq)	819	48	4	871

6.2.5 Summary of LCA

A summary of the primary energy use of the lightweight building for different floor panels, together with the primary energy use for the concrete building is presented in Figure 6.3. It is seen that the concrete building has the lowest total primary energy, but the highest non-renewable primary energy.

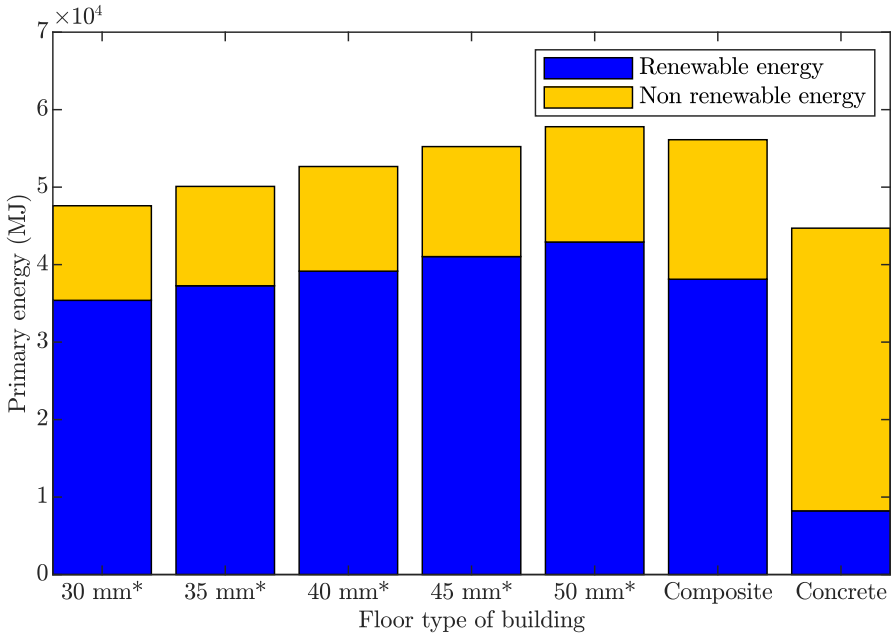

Figure 6.3: Primary energy use for the investigated buildings. *Ply thickness of the CLT floor panels.

Presented in Figure 6.4 is the GWP for the different buildings. The concrete building has a significantly higher GWP compared with the other alternatives.

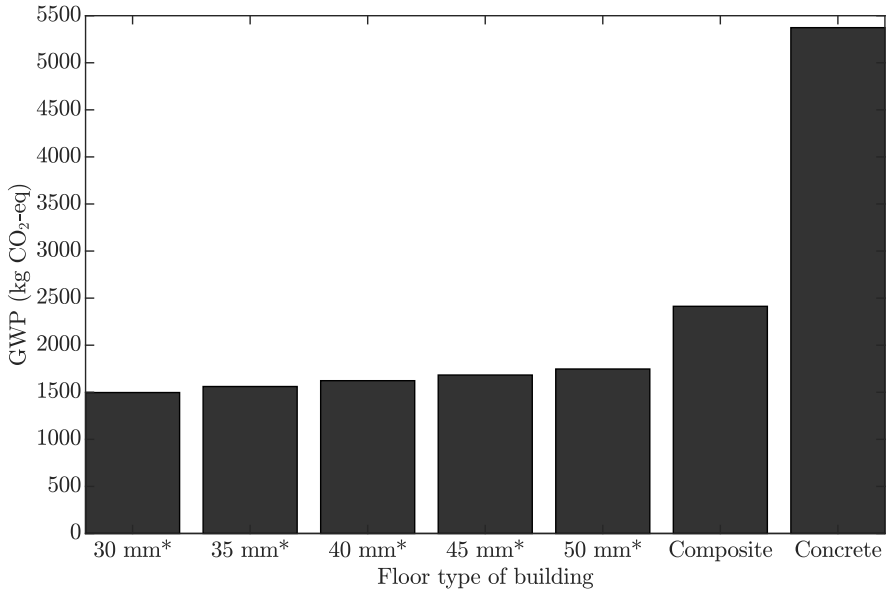

Figure 6.4: GWP for the investigated buildings. *Ply thickness of the CLT floor panels.

6.3 Numerical model

The numerical model was created as a 2D FE model in Abaqus consisting of a 200 m x 60 m layered ground divided into soil at the surface and bedrock underneath. In

the middle of the surface, a three-storey building was modelled. Between the building and ground, as well as the different parts of the building, tie constraints were used to model full interaction between the parts. A vertical unit point load was placed 20 m from the edge of the building and a frequency sweep was performed between the frequencies 1 Hz–80 Hz using a steady-state direct analysis.

6.3.1 Ground model

The ground model consists of a 20 m deep layer of soil and a 40 m deep layer of bedrock. The materials were modelled as homogeneous, isotropic and linear elastic. Analyses were performed for both a stiff soil, and a soft soil with a lower Young's modulus. The material parameters used for the soils are presented in Table 6.8. The material properties used for the bedrock are presented in Table 6.9.

Table 6.8: Material properties used for the ground.

(a) Material properties used for the stiff soil.

Stiff soil	
Density(kg/m^3)	2000
E (MPa)	500
v (-)	0.48
$Loss\ factor$ (-)	0.1

(b) Material properties used for the soft soil.

Soft soil	
Density (kg/m^3)	2000
E (MPa)	150
v (-)	0.48
$Loss\ factor$ (-)	0.1

Table 6.9: Material properties used for the bedrock.

Bedrock	
Density (kg/m^3)	2500
E (MPa)	10000
v (-)	0.4
$Loss\ factor$ (-)	0.04

As the ground extends further than the boundaries of the model, 5-node plane strain solid continuum infinite (CINPE5R in Abaqus) elements were used along the non-surface edges of the ground. This is done in order to minimise unwanted reflections along the edges. The element size used for the mesh is 0.5 m x 0.5 m in order to properly resolve the wavelength of the propagating waves within the frequency range considered. Presented in Figure 6.5 is a visualisation of the mesh used.

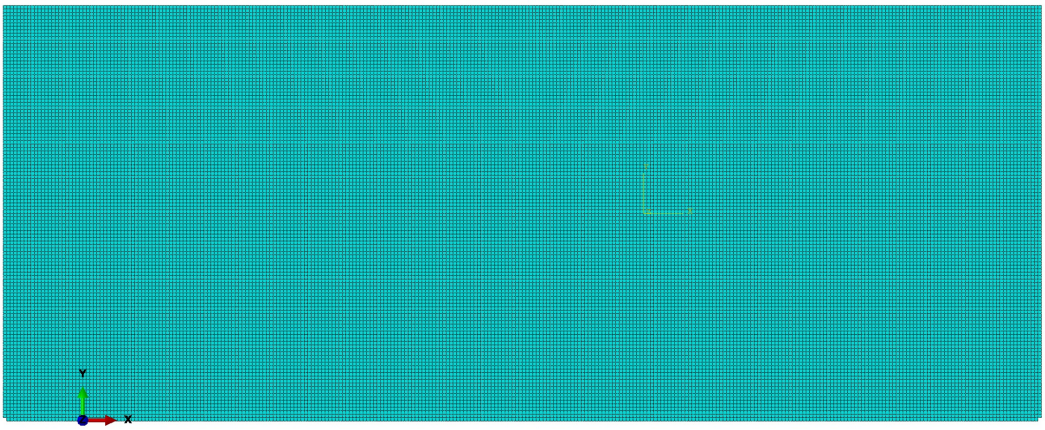

Figure 6.5: Visualisation of the FE mesh used for the ground.

6.3.2 Building model

The building is modelled with 8-node plane strain elements (CPE8R in Abaqus) with element size 0.1 m x 0.1 m. The material properties used for the glulam and C30 concrete are shown in Table 6.10. The floor panels are modelled using the same material properties presented in Table 5.12.

Table 6.10: Material properties used for C30 concrete and GL32h glulam.

(a) Material properties used for C30.

Concrete C30	
Density(kg/m^3)	2400
E (MPa)	32 000
v (-)	0.2
Loss factor (-)	0.03

(b) Material properties used for Gl32h glulam.

GL32h	
Density(kg/m^3)	430
E_L (MPa)	13700
E_R (MPa)	460
E_T (MPa)	460
G_{LR} (MPa)	850
G_{LT} (MPa)	850
G_{RT} (MPa)	23
v_{LR} (-)	0.38
v_{LT} (-)	0.51
v_{TR} (-)	0.31
Loss factor (-)	0.06

The floor panels of the building are either modelled using a homogeneous concrete floor panel or CLT floor panel divided into seven different plies with each ply orientated perpendicular to the adjacent. The material properties used for the floor panels those shown in Table 5.12. The numerical model of the building is shown in Figure 6.6.

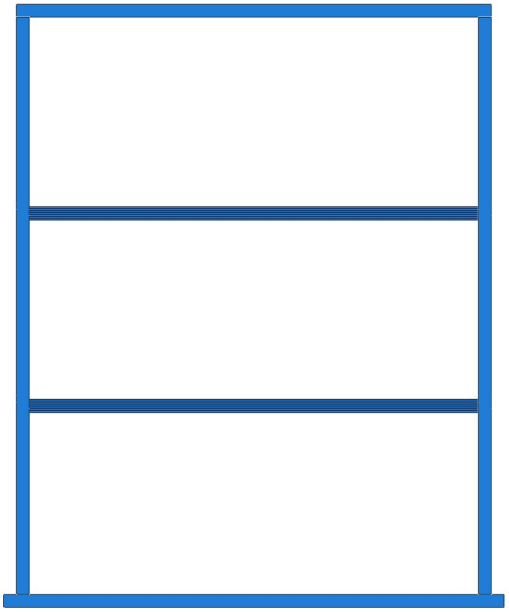

Figure 6.6: Visualisation of the building which is modelled.

6.4 Parameter study

The parameter study was performed by investigating the response at all floor panels for the different buildings placed on either the soft soil, or the stiff soil. For all investigated cases, the highest RMS velocities and RMS accelerations were found at the third floor, thus only the vibration of the third floor is presented. The velocity response for the first and second floor can be found in Appendix B.

6.4.1 Velocity between 1 Hz–80 Hz

Presented in Figure 6.7 and Figure 6.8 are the magnitudes of the complex velocity amplitudes for the third floor panel midpoint for the buildings placed on stiff soil and soft soil, respectively. For the stiff soil, a strong resonance peak for all buildings is seen around 8 Hz. The resonance peaks are shifted forwards with increasing ply thickness and a reduced amplitude is seen. For the soft soil, two resonance peaks are seen between the frequencies 5 Hz–11 Hz. The amplitude was generally lower when a soft soil was used.

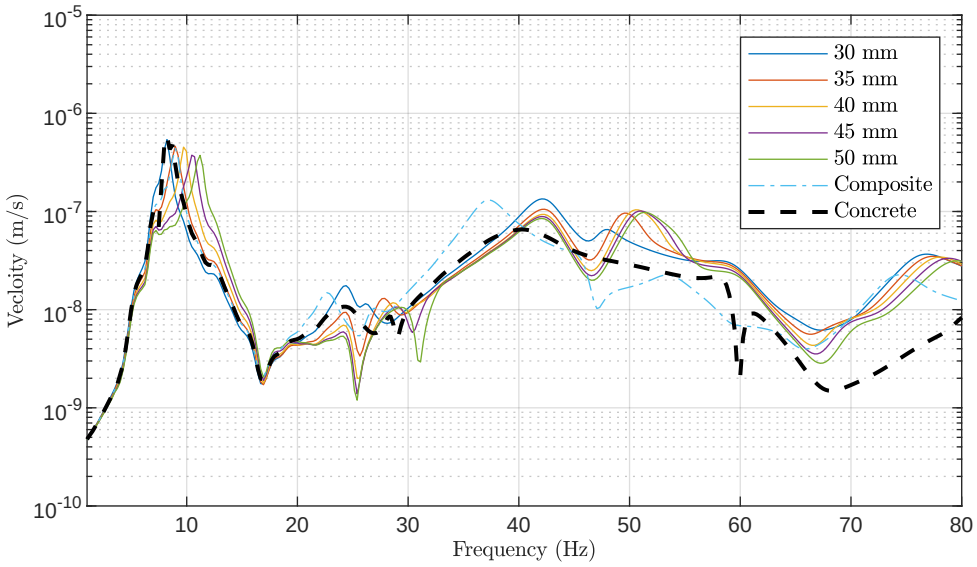

Figure 6.7: Velocity response of the different buildings on a stiff soil, evaluated at the midpoint of the third floor.

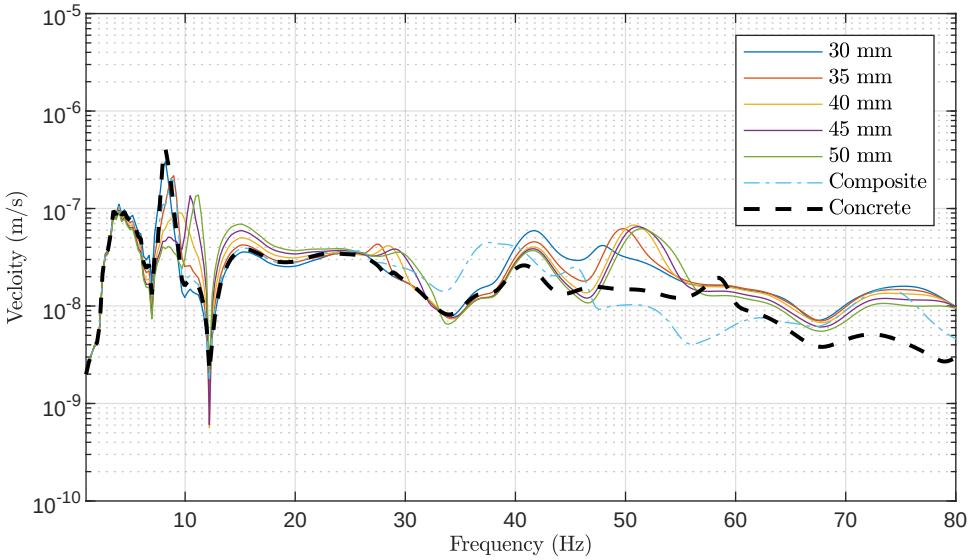

Figure 6.8: Velocity response of the different buildings on a soft soil, evaluated at the midpoint of the third floor.

The vertical velocities amplitudes of the different soils are presented in Figure 6.9 and Figure 6.10 for the analyses of the concrete building and the lightweight building, respectively. The response of the soil was evaluated between the load and the building, 0.1 m from the edge of the foundation. It can be observed that the frequencies of the first velocity peaks of the third floor largely correspond with the first velocity peaks of the soil as it coincides with the eigenfrequencies of the buildings. For example, a resonance peak is found around 3 Hz for the building on a soft soil, which is not seen for the buildings on the stiff soil due to the first velocity peak of the stiff soil being almost 9 Hz. For the soft soil, a strong peak for the concrete floor panel is seen at a dip for the velocity of the soil, while lower peak, in relation to the concrete floor

panel, is seen for the 50 mm CLT floor panel where a peak in velocity of the soft soil is seen. This shows that the velocities of the floor panels are not solely dependant on the magnitude of the velocity of the soil. A difference between the responses of the soils can also be seen depending on the building investigated, with the stiff soil being more sensitive to the type of building.

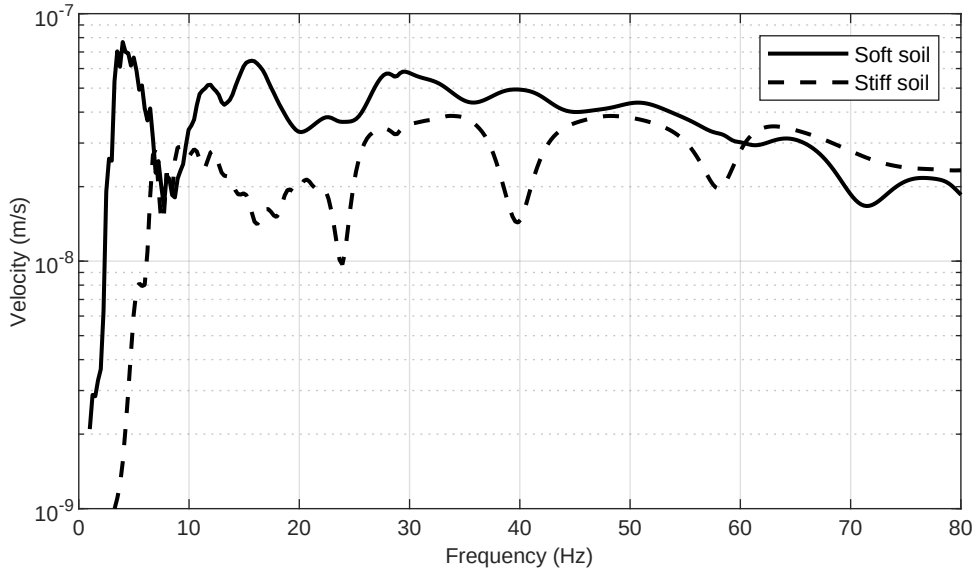

Figure 6.9: Vertical velocity of the stiff and soft soil at the surface 0.1 m from the foundation of the concrete building.

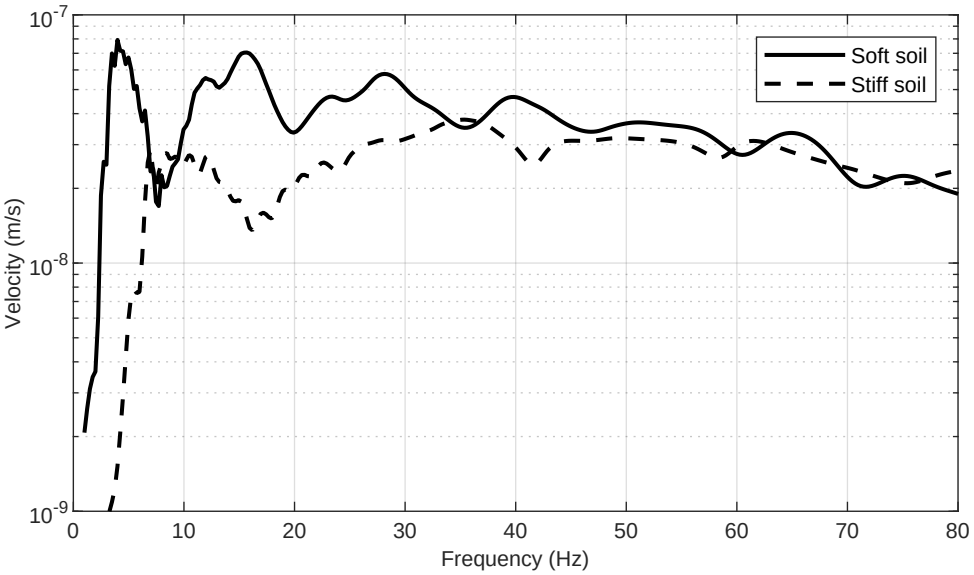

Figure 6.10: Vertical velocity of the stiff and soft soil at the surface, 0.1 m from the foundation of the 30 mm ply thickness lightweight building.

For the comparison between the lightweight buildings and the reference concrete building presented in Figure 6.11 and Figure 6.12 for stiff and soft soil, respectively, the RMS of the FRF was calculated and divided by the RMS of the concrete building.

For both soils, the concrete building had the highest RMS velocity. When placed on the stiff soil, the 50 mm CLT floor panel has the lowest RMS velocity. When placed on the soft soil, the 40 mm CLT has the lowest RMS velocity. Having the buildings placed on the soft soil shows a lower RMS velocity of the CLT floor panels, in relation to the concrete building, compared with having the buildings placed on the stiff soil. The RMS velocity of the composite floor panel, in relation to the concrete floor panel is largely unaffected by the type of soil. For the soft soil, the RMS velocities of the CLT floor panels were decreased with increasing ply thickness up to a thickness of 40 mm, where a further increase in thickness proved to result in a higher RMS velocity. This phenomenon is further discussed in Section 7.1.2.

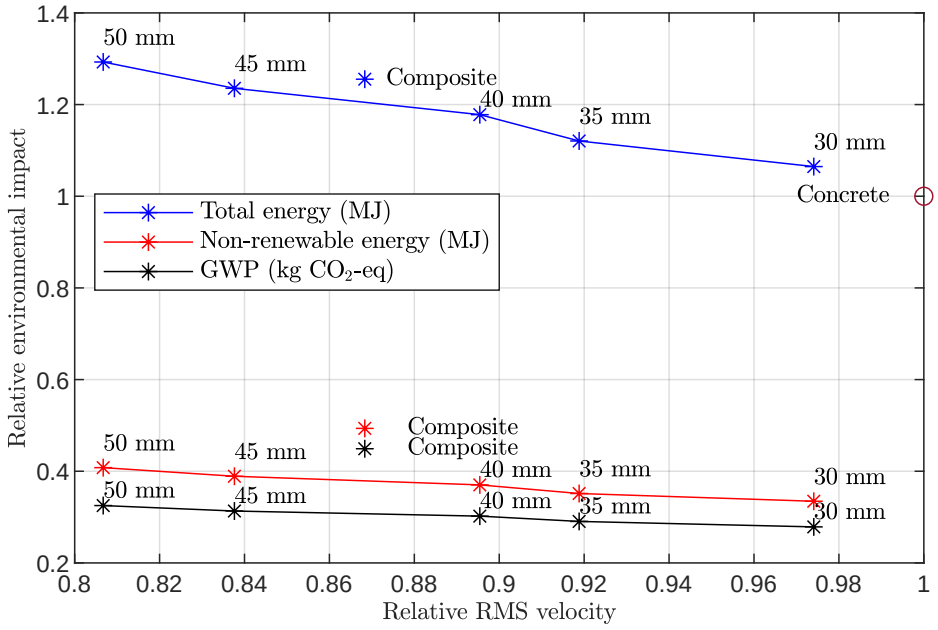

Figure 6.11: Environmental impact and RMS velocity of the lightweight buildings in relation to the concrete building for the stiff soil.

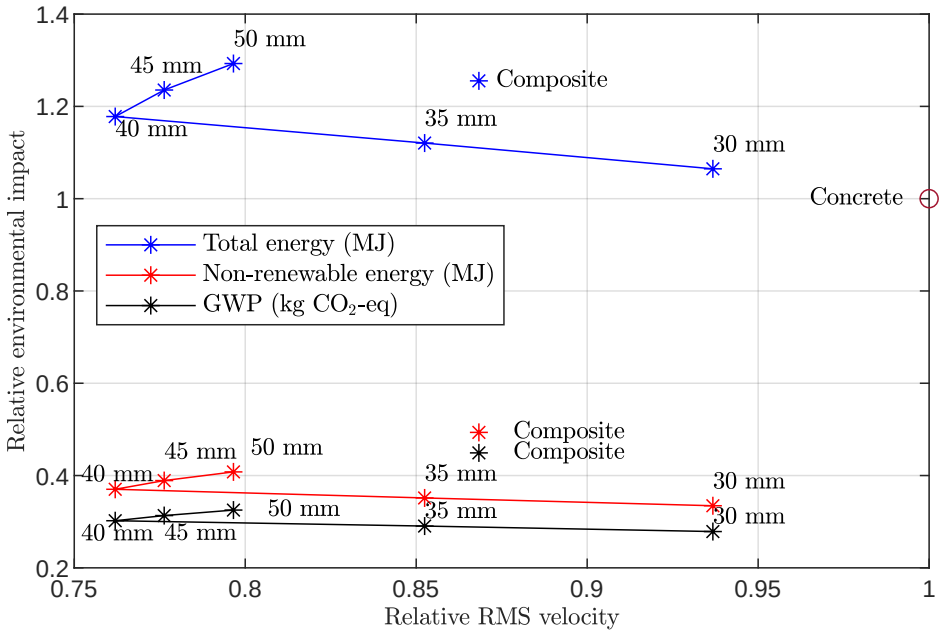

Figure 6.12: Environmental impact and RMS velocity of the lightweight buildings in relation to the concrete building for the soft soil.

6.4.2 Weighted acceleration between 1 Hz–80 Hz

For the weighted acceleration, the complex acceleration amplitude was weighted according to the weighting spectrum in Section 3.2.2. Presented in Figure 6.13 and Figure 6.14 are the weighted accelerations in the midpoint of the third floor for a stiff soil and a soft soil, respectively. A similar response is seen here as for the evaluation of the unweighted velocity.

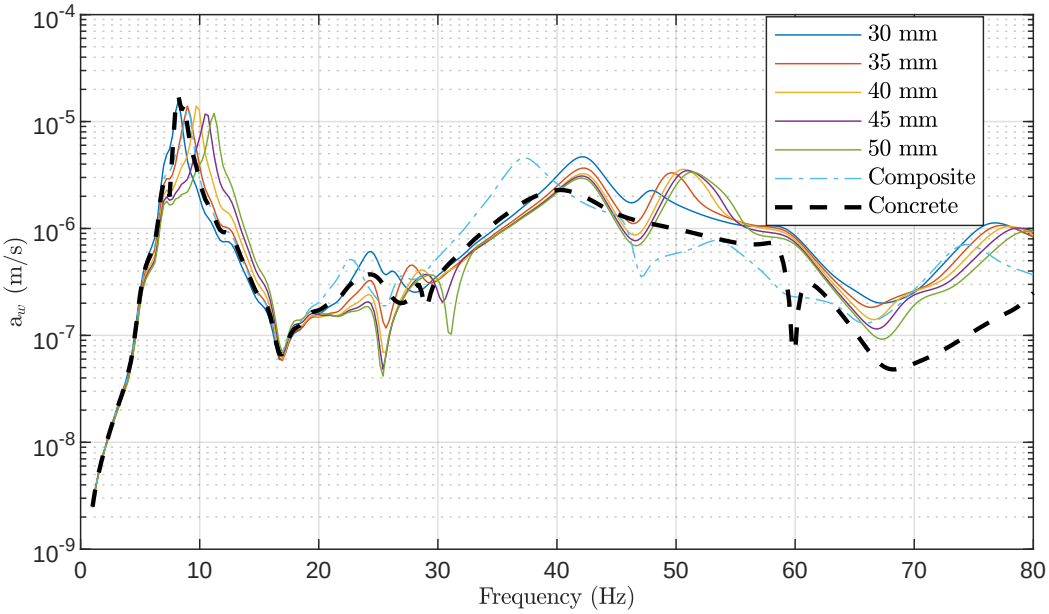

Figure 6.13: Weighted acceleration for the different buildings on a stiff soil, evaluated at the third floor midpoint.

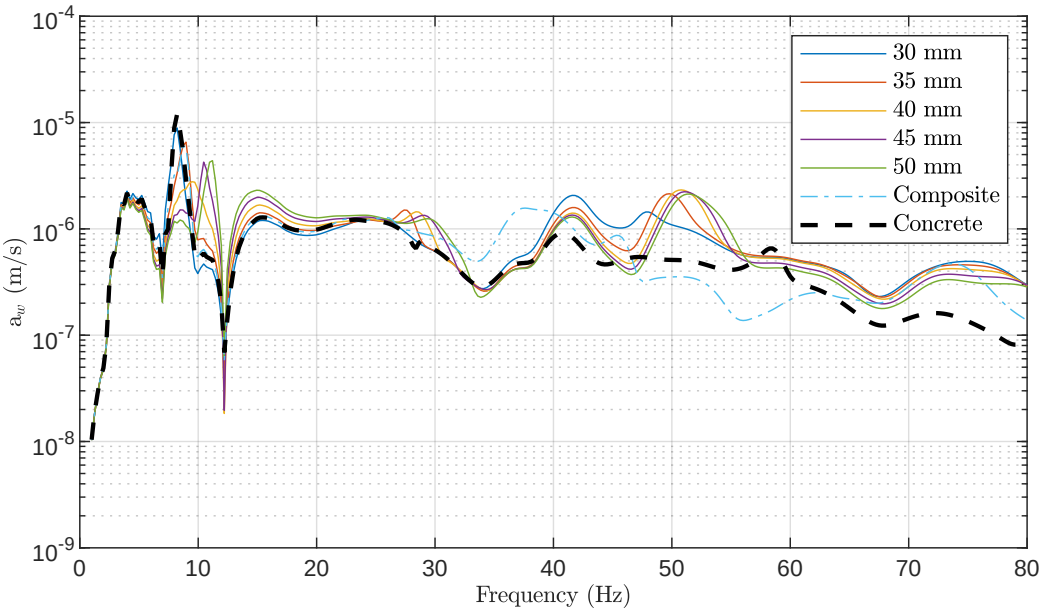

Figure 6.14: Weighted acceleration for the different buildings on a soft soil, evaluated at the third floor midpoint.

Presented in Figure 6.15 and Figure 6.16 is a comparison between the lightweight buildings and the reference concrete building. The relative weighted RMS acceleration is the RMS of the acceleration FRF divided with the corresponding RMS for the reference concrete building. Only the lightweight building on a stiff soil with a 30 mm ply thickness CLT floor panel had a higher weighted RMS acceleration compared with the concrete building. For the stiff soil, the 50 mm ply thickness CLT floor panel had the lowest relative RMS acceleration. For the soft soil, the same result is seen here as for the velocity where the 40 mm ply thickness CLT floor panel had the lowest relative RMS acceleration as the RMS increased with a thicker floor panel.

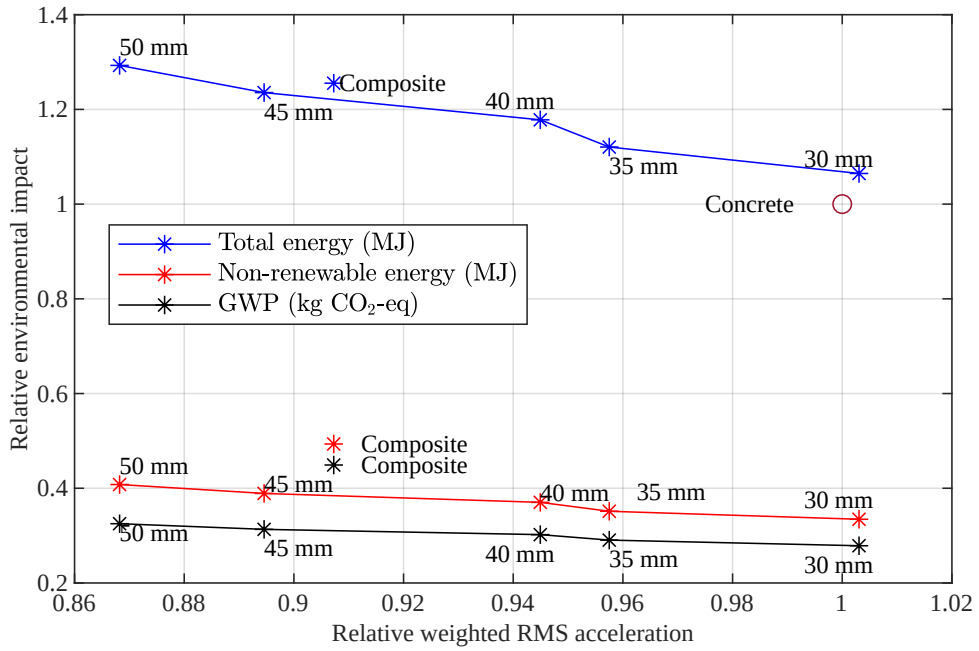

Figure 6.15: Environmental impact and relative weighted RMS acceleration of the lightweight buildings in relation to the concrete building for the stiff soil.

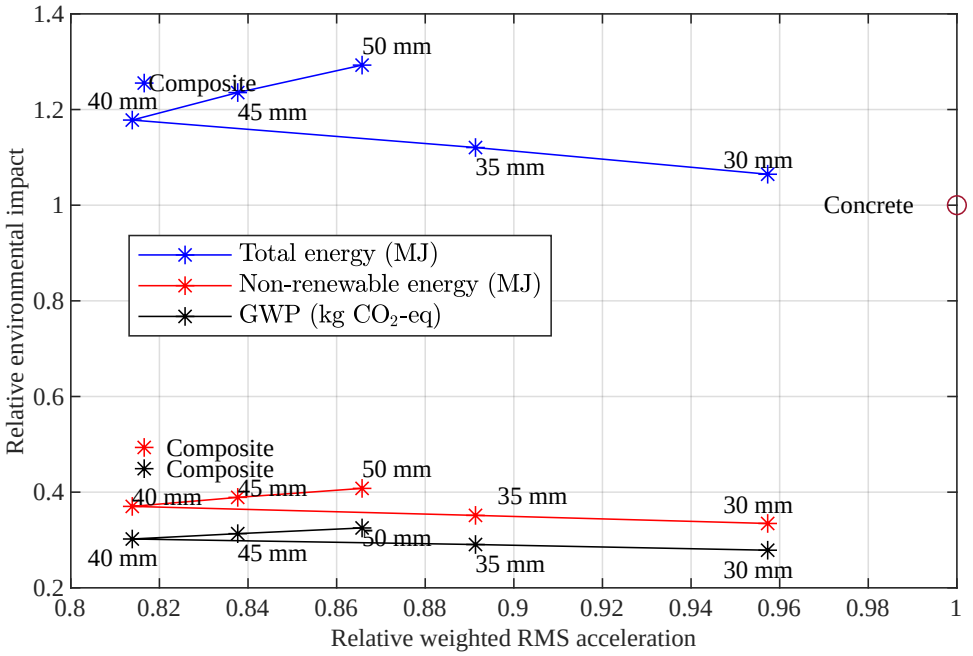

Figure 6.16: Environmental impact and relative weighted RMS acceleration of the lightweight buildings in relation to the concrete building for the soft soil.

7 Discussion and conclusions

In this chapter, the results found regarding LCA and vibroacoustic performance of the investigated floors and buildings are discussed. A discussion of the evaluation methods used to present the vibroacoustic performance and LCA is also presented. Further, the main conclusions from this report are presented together with proposals for future work.

7.1 Discussion

7.1.1 Reference case 1: floor panel

Looking at the results of environmental impact, the production of CLT showed to be an energy demanding process with a higher total energy demand than the concrete floor panel for the thickest CLT floor panels. Most of the energy consumed is from renewable energy sources and regarding non-renewable energy and GWP, the choice of a CLT floor panel would be a significantly better choice. The composite floor panel had a higher non-renewable energy and GWP compared to any CLT floor panel but a lower GWP compared to a concrete floor panel.

When considering the steady-state dynamic analysis, the concrete floor panel provides a significantly better low-frequency vibroacoustic performance. Increasing the thickness of the CLT floor panel generally improved the performance, although within the analysed thicknesses never being close to the same level as the concrete floor panel. The investigated thicknesses of the CLT floor panel had 3.5–5.7 times higher RMS velocity and 40–52 times higher ERP than the concrete floor panel in terms of RMS values in the frequency ranges considered. Increasing the ply thickness above 40 mm had a low effect on the ERP. The composite floor panel had a better performance with only twice the RMS velocity but almost 50 times higher ERP in relation to the concrete floor panel. The ERP of the concrete floor panel was much lower than any other floor panel indicating that the vibration across the whole concrete floor panel (as opposed to only considering point P2 as for the RMS), and the resulting ERP is significantly lower. It is not possible to draw any conclusions on how this difference in ERP affects the disturbance, or sound class rating of a floor panel as only a unit load was applied and no calculation of the sound pressure level was made.

When considering footsteps and applying weighting to the response, increasing the ply thickness from 40 mm to 45 mm showed to result in worse performance for all evaluations. An explanation to this observation is that the eigenfrequencies are being shifted towards frequencies where the footstep loading is high. The response also proved to be sensitive to the walking frequency. When applying a walking frequency of 1.83 Hz, a significantly higher RMS acceleration for the 45 mm ply thickness was

seen when compared to a walking frequency of 2 Hz. A load pulse of a footstep varies depending on factors such as the surface and what shoes the subject is wearing. When adding a strong heelstrike in the beginning of a footstep, a significant increase in the vibration and a shift in the balancing of the floor panels was seen. This makes the prediction of the vibration, regarding force applied to floor panel from a footstep somewhat complicated. Together with the sensitivity to the walking frequency, and the use of only three different walking frequencies in the dissertation, the result is somewhat inconclusive regarding the general performance of the CLT floor panels. To account for variations in walking frequencies, analysing the response across a wide range of the probable walking frequencies by, for example, using a Monte Carlo simulation would provide a better estimation of the vibroacoustic performance.

When applying the base curve from ISO 10137, only the CLT floor panels with ply thicknesses between 30 mm–45 mm exceeded the base curve limits at some frequencies. Provided these results, when considering satisfactory vibrations in regards to whole-body vibration, using a CLT floor panel with 50 mm ply thickness, or a composite floor panel was shown to provide a good performance. This highlights the importance of considering requirements and target levels, which are carefully chosen, when evaluating the relative performance of different floor panels and building designs.

A conclusion of these analyses is that while CLT floor panels of all thicknesses have a lower non-renewable energy consumption and GWP in relation to concrete, the vibroacoustic performance was worse; the exception being the CLT floor panel with 50 mm ply thickness, which gave zero exceedance of the vibration base curve used in the analyses. The composite floor panel provided the best balance between the environmental impact and vibroacoustic performance in relation to concrete. The composite floor panel having approximately half the non-renewable energy consumption and GWP in relation to concrete, indicates that further adjustments could be made, such as a thicker concrete layer in order to achieve a similar vibroacoustic performance, while still having a lower non-renewable energy consumption and GWP in relation to a concrete floor panel.

Investigation of a 150 mm and a 250 concrete floor panel showed that the 150 mm concrete floor panel had a worse performance in regards to whole-body vibration in relation to the composite, and roughly equal to the 50 mm ply thickness CLT floor panel. Assuming the same EE and GWP per unit of mass as the 200 mm concrete floor panel, the 150 mm concrete floor panel still had a higher non-renewable energy and GWP in relation to the floor panels containing timber. The 250 mm had a significantly better performance compared with any other floor panel, while further having a higher total energy use, non-renewable energy use and GWP. This suggests having a 50 mm CLT floor panel, or a composite floor panel is a preferable alternative to a 150 mm concrete in regards to all investigated aspects, except for total energy use. An alternative to the RDF type concrete floor panels are hollow core floor panels, not investigated in this report, which could provide a better balance between the vibroacoustic performance and environmental impact. Hollow core floor panels could provide a good vibroacoustic performance having the material properties of concrete, while having a significantly lower environmental impact in relation to an RDF floor panel due to its lower mass.

7.1.2 Reference case 2: building exposed to external loading

For the velocity of the floor panels, all lightweight buildings had a lower RMS velocity in relation to the concrete building. The lightweight buildings had a significantly lower GWP and consumption of non-renewable energy, while the total energy demand for all investigated lightweight buildings were higher in relation to the concrete building. When applying the weighting spectrum to the acceleration, the relative weighted RMS acceleration was lower than the concrete building in all investigated cases except for the lightweight building on the stiff soil with 30 mm CLT floor panels. The relative weighted RMS accelerations were slightly higher for the lightweight building compared to the unweighted relative RMS velocity. Having the building placed on a soft soil favoured the choice of a lightweight building. Increasing the ply thickness of the CLT floor panels past 40 mm, did however increase the RMS velocity and RMS acceleration. Comparing the vertical velocity of the soft soil and the response of the floor panels shows that the second amplitude peak of the soil coincides with a resonance peak of the 45 mm and 50 mm ply thickness floor panels but not in the other investigated floor panels. This suggests that having high amplitudes of the propagating waves coinciding with the eigenfrequencies of the building and its element increases the velocity at certain frequencies, thus increasing the RMS velocity and RMS acceleration when having a soft soil. A similar explanation can be given to the concrete building having the highest RMS velocity and RMS acceleration with the large response as the frequency content of the ground vibration coincides with the fundamental frequency of the concrete building. For the weighted acceleration, this becomes more prevalent if the fundamental frequency occurs at a frequency where humans are more sensitive.

A conclusion of these analyses is that the vibration performance of the buildings is sensitive to the matching between its eigenfrequencies, the frequency content of the propagating waves, and the frequency dependence of the human sensitivity. The fundamental frequency varies due to factors such as the dimensions of a building. The content frequency of the propagating waves depend on the soil type, load, and to some extent the building placed on it. This makes it difficult to draw any general conclusions concerning the vibration performance in regards to the choice of material as it becomes very much case specific. The general trend for the lightweight building with CLT floor panels, is that an increased thickness lowers the vibration. Regarding environmental impact, the total energy consumption for the lightweight buildings is higher, compared to the concrete building. The non-renewable energy and GWP is significantly lower for the lightweight building in relation to the concrete building.

7.1.3 Evaluation of vibroacoustic performance

Regarding whole-body vibration, a conclusion of the literature study is that using a weighted acceleration is a recommended method in order to account for the frequency-dependant sensitivity a human has to whole-body vibrations. The human sensitivity to whole-body vibrations is very much dependant on the particular use of the building, for example whether it is used for industrial work, or for a dwelling, and applying the base curve given in ISO 10137 offers a method for assessing acceptable vibration levels in different situations. Using the weighted acceleration and the base curve for a realistic load case such as footsteps can thus give an indication whether an occupant

will be disturbed by the vibrations or not. When the base curve is not appropriate due to the ratio between the peak value and the RMS value, as suggested in ISO 10137, comparing the VDV with given thresholds can instead give guidance on acceptable vibrations.

In this dissertation, the approach of calculating the RSS for the exceedance of the base curve was chosen in order to quantify the performance as any acceleration lower than the base curve limits would not contribute to any disturbance. By using this approach, balancing the vibration performance becomes a question of reaching acceptable levels of vibration, rather than simply comparing the vibration magnitudes. This was shown to be very important since some floor panels, under the footstep load case, did not exceed the base curve.

The amplitude of the resonance peaks has a significant influence on the vibroacoustic performance as the evaluation metrics were calculated as RMS, VDV (being a root-mean-quad), or exceedance of the base curve where the exceedance was only found at the resonance peaks. For the weighted accelerations, the frequencies of the resonance peaks also were important as the high frequency peaks are reduced by the weighting. When evaluating the vibroacoustic performance for an external load, the matching between the eigenfrequency of the building and the frequency content of the ground vibrations proved to significantly affect the vibration in the floors of the building. It is therefore important to consider this in analyses of external loads designing a building as it can be very much case specific, i.e. no general conclusion can be made regarding different buildings materials.

7.1.4 Evaluation of EE and GWP

In this report the EE and GWP considered in the analysis showed that the consumption of non-renewable energy and the GWP was significantly lower for timber. The total energy consumption proved to be high for timber, and the relevancy of this indicator should be considered in the design. For the renewable energy use of timber, the EPDs and databases did not specify the energy source. The literature study suggested that drying of timber was a significant contributor to the energy consumption, with most of this energy being extracted from by-products of sawing, thus being renewable. An investigation of the environmental impact due to the energy production was not conducted, but could be important when considering the importance of the total energy consumption.

In regards to timber, it is important to consider the type of GWP used in the calculations as the total GWP often becomes a negative value due to the uptake of carbon dioxide during the growth of the tree. This carbon dioxide is then released if the timber is decomposed and thus it depends on the end-of-life use of the product.

While the embodied energy is mostly accumulated during module A, it does include any addition to the embodied energy during renovation, refurbishments or deconstruction in the later stages of the building. This may change the relation of the embodied energy between timber and concrete as the extent of any refurbishment or waste processing after deconstruction can vary.

The accuracy of data for an LCA is important to consider. While published EPDs of a specific product generally can be regarded as accurate, containing data provided by the manufacturer, the EPD used for CLT for example, contains average data of Swedish forestry for the supply of wood. In this dissertation, German average values were used for these modules giving an uncertainty as geographical variations exist.

Embodied energy and GWP for transport and construction varies on a case basis, data on the lorries and machinery for example would have to be collected in order for the data to be accurate. The transport distance is also an important factor to consider for the LCA. In this dissertation, a transport distance of 200 km was used. Module A4 for this distance stood for 12.6 % and 3.6 % of the total energy consumption for the concrete floor panel and the CLT floor panels, respectively. Regarding the GWP, module A4 was 7.5 % and 10 % of the total GWP for the concrete floor panel and the CLT floor panels, respectively. Having a larger transport distance from the factory to the construction site could thus be a dominating factor for large distances, especially when considering different materials with different distances from the corresponding factories. Having a very large transport distance of CLT in relation to a concrete alternative, for example, could make the choice of concrete a more favourable in regards to the environmental impact.

7.2 Main conclusions

Presented here are the main conclusions of the dissertation:

- A CLT floor panel, or a composite floor panel has a significantly lower non-renewable primary energy use and GWP compared with a concrete floor panel. However, the EE (total primary energy use) was similar, or higher than concrete.
- A composite floor panel or a 50 mm ply thickness CLT floor panel provided a relatively good vibroacoustic performance in relation to reinforced concrete when subjected to a footstep load. In general, increasing the thickness of the CLT floor panel resulted in a better performance.
- A lightweight building exposed to an external load had a better vibroacoustic performance for the investigated case compared to a concrete building. Of the investigated buildings, having 50 mm ply thickness CLT floor panels provided the best performance on a stiff soil. Having 40 mm ply thickness CLT floor panels provided the best performance on a soft soil.
- When considering an external load, it is important to consider the eigenfrequencies of the building and how it matches the frequency content of the propagating waves in the soil. This makes analyses of optimal material selection case specific and highly dependent on soil properties.
- When considering a footstep load, it is important to consider variations in the load spectrum and walking frequencies, for example by Monte Carlo simulations. This is due to the varying relative vibroacoustic performance observed for the floor panels, potentially affecting the optimal floor panel choice in the balancing.

- Using the base curve in ISO 10137 with a weighted acceleration provides a good method of determining acceptable limits in regards to whole-body vibrations. Rather than using absolute values, the base curve can be used for assessing acceptable vibration levels based on human annoyance.
- Using databases with generic data introduces an uncertainty into the LCA. When using EPDs, it can for example be difficult to find the source of the energy as it could be of interest whether it is from electricity or thermal energy extracted from waste products during manufacturing.

7.3 Future work

Presented in this section are some proposals for future work based on the study performed in this dissertation.

- Further study regarding footstep pulses can be performed, such as varying load spectra depending on the walking rate, floor material and footwear. Analyses can also be performed for a moving load, simulating a person walking across the floor.
- A more extensive analysis regarding a building exposed to external loads can be performed. This can, for example include applying a realistic load from a vehicle, rather than using a unit load. The response can for this load be compared with the base curve or VDV in similar way as for the first reference case. Further analyses can also be performed by altering the dimensions of the building and investigating the effects of different sizes of a building.
- Performing an LCA considering the end of life stage, and considering the effects of reuse or recycling can be performed to investigate how sensitive the results are to the last stages of the life cycle.
- Analyses of structure-borne sound through modelling transmission to the receiving room can be performed to further investigate the acoustic performance of different materials in buildings.

Bibliography

[1] R. Brandner, G. Flatscher, A. Ringhofer, G. Schickhofer and A. Thiel. "Cross laminated timber (CLT): overview and development." In: *European Journal of Wood Wood Products / Holz als Roh- und Werkstoff* 74.3 (2016), pp. 331 –351.

[2] OECD. *Environmentally Sustainable Buildings*. 2003, p. 196.

[3] Miller Sabbie A, Horvath Arpad and Monteiro Paulo J M. "Readily implementable techniques can cut annual CO2 emissions from the production of concrete by over 20%." In: *Environmental Research Letters* (2016), p. 1.

[4] Maria Lúcia Machado Duarte, Priscila Albuquerque de Araújo, Frederico Catone Horta, Sara Del Vecchio and Lucas Augusto Penna de Carvalho. "Correlation between weighted acceleration, vibration dose value and exposure time on whole body vibration comfort levels evaluation". In: *Safety Science* (2018), pp. 218–224.

[5] Robert Crawford. *Life Cycle Assessment in the Built Environment.* Florence: CRC Press LCC, 2011.

[6] Svenskt trä. *Att välja trä : en faktaskrift om trä.* Stockholm: Svenskt trä, 2020.

[7] Swedish standards institute. *SS-EN 15804:2012+A2:2019. Sustainability of construction works - Environmental product declarations - Core rules for the product category of construction products*. Stockholm: SIS, 2019.

[8] Swedish standards institute. *SS-EN 15978. Sustainability of construction works – Assessment of environmental performance in buildings – Calculation methods.* Stockholm: SIS, 2011.

[9] Evert Nieuwlaar. "Life Cycle Assessment and Energy Systems". In: *Encyclopedia of Energy*. Ed. by Cutler J. Cleveland. New York: Elsevier, 2004.

[10] Manish K. Dixit. "Life cycle embodied energy analysis of residential buildings: A review of literature to investigate embodied energy parameters". In: *Renewable and Sustainable Energy Reviews* 79 (2017), pp. 390–413.

[11] Leif Gustavsson and Anna Joelsson. "Life cycle primary energy analysis of residential buildings." In: *Energy and Buildings* 42 (2010), pp. 210 –220.

[12] *Climate change 2013 : the physical science basis : Working Group I contribution to the fifth assessment report of the Intergovernmental Panel on Climate Change.* Cambridge University Press, 2013.

[13] Martin Erlandsson. *LCA for Setra glulam*. Tech. rep. Stockholm, 2018.

[14] Deborah N. Huntzinger and Thomas D. Eatmon. "A life-cycle assessment of Portland cement manufacturing: comparing the traditional process with alternative technologies". In: *Journal of Cleaner Production* 17.7 (2009), pp. 668–675.

[15] Martin Erlandsson, Malmqvist Tove, Nicolas Francart and Johnny Kellner. *Minskad klimatpåverkan från nybyggda flerbostadshus. LCA av fem byggsystem. Underlagsrapport*. 2018.

[16] Ola Flodén. “Vibration transmission in lightweight buildings: numerical prediction models”. PhD thesis. 2016.

[17] Peter Persson. “Vibrations in a Built Environment”. PhD thesis. 2016.

[18] Osama A. B. Hassan and John Laurence Davy. “Building Acoustics and Vibration—Theory and Practice.” In: *Journal of the Acoustical Society of America* 127.2 (2010), pp. 1168 –1169.

[19] Juan Negreira. “Vibroacoustic Performance Of Wooden Buildings”. PhD thesis. 2016.

[20] Swedish standards institute. *SS-EN ISO 717-1:2020. Acoustics — Rating of sound insulation in buildings and of building elements — Part 1: Airborne sound insulation.* Stockholm: SIS, 2020.

[21] Swedish standards institute. *SS-EN ISO 717-2:2020. Acoustics — Rating of sound insulation in buildings and of building elements — Part 2: Impact sound insulation.* Stockholm: SIS, 2020.

[22] Fredrik Ljunggren, Christian Simmons and Rikard Öqvist. “Correlation between sound insulation and occupants’ perception: Proposal of alternative single number rating of impact sound, part II.” In: *Applied Acoustics* 123 (2017), pp. 143 –151.

[23] Swedish standards institute. *ISO 2631-1. Mechanical vibration and shock – Evaluation of human exposure to whole-body vibration – Part 1: General requirements.* Stockholm: SIS, 1997.

[24] A.L. Smith, Stephen Hicks, Paul Devine and Steel Britain. *Design of Floors for Vibration: A New Approach.* Ascot: The Steel Construction Institute, 2007, p. 114.

[25] Swedish standards institute. *SS-ISO 2631-2 Mechanical vibration and shock - Evaluation of human exposure to whole-body vibration. Part 2: Vibration in buildings (1 Hz to 80 Hz).* 2003.

[26] Swedish standards institute. *ISO 10137:2007. Bases for design of structures – Serviceability of buildings and walkways against vibrations.* 2007.

[27] Swedish standards institute. *SS 25267:2015. Byggakustik - Ljudklassning av utrymmen i byggnader - Bostäder.* Stockholm: SIS, 2015.

[28] Swedish standards institute. *SS 25268:2007+T1:2017. Acoustics — Sound classification of spaces in buildings — institutional premises, rooms for education, preschools and leisure-time centres, rooms for office work and hotels.* Stockholm: SIS, 2008.

[29] Niels Saabye Ottosen and Hans Petersson. *Introduction to the finite element method.* New York: Prentice Hall, 1992.

[30] V. Racic, A. Pavic and J.M.W. Brownjohn. “Experimental identification and analytical modelling of human walking forces: Literature review.” In: *Journal of Sound and Vibration* 326.1 (2009), pp. 1 –49.

[31] Svensk Betong. *Massiva bjälklagsplattor (RD & RD/F).* 2021. URL: https://www.svenskbetong.se/bygga-med-betong/bygga-med-prefab/statik/massiva-bjalklagsplattor-rd-rd-f.

[32] Svenskt trä. *KL-trähandbok : fakta och projektering av KL-träkonstruktioner.* Stockholm: Svenskt trä, 2017.

[33] The Norwegian EPD Foundation. *Environmental product declaration — Massivt förspänt bjälklag — Strängbetong AB.* Oslo: The Norwegian EPD Foundation, 2019.

[34] The Norwegian EPD foundation. *Environmental product declaration — KL-tre— Martinsons Såg AB.* Oslo: The Norwegian EPD Foundation, 2019.

[35] Federal Ministry of the Interior, Building and Community. *ÖKOBAUDAT.* URL: https://www.oekobaudat.de/en.html.

[36] The Norwegian EPD Foundation. *Environmental product declaration. Limtre.* Oslo: The Norwegian EPD Foundation, 2021.

[37] The Norwegian EPD Foundation. *Environmental product declaration. Betongpelare RP.* Oslo: The Norwegian EPD Foundation, 2019.

Appendix A

Weighted frequency spectra

Presented in Figure A.1 and Figure A.2 are the weighted frequency acceleration spectra for a walking frequency of 1.83 Hz, and 2.17 Hz respectively. The RMS values presented for the CLT floor panels, the composite floor panel, and the 200 mm thick concrete floor panel are used for the calculation of the average spectra for the three investigated walking frequencies presented in Section 5.4.2.

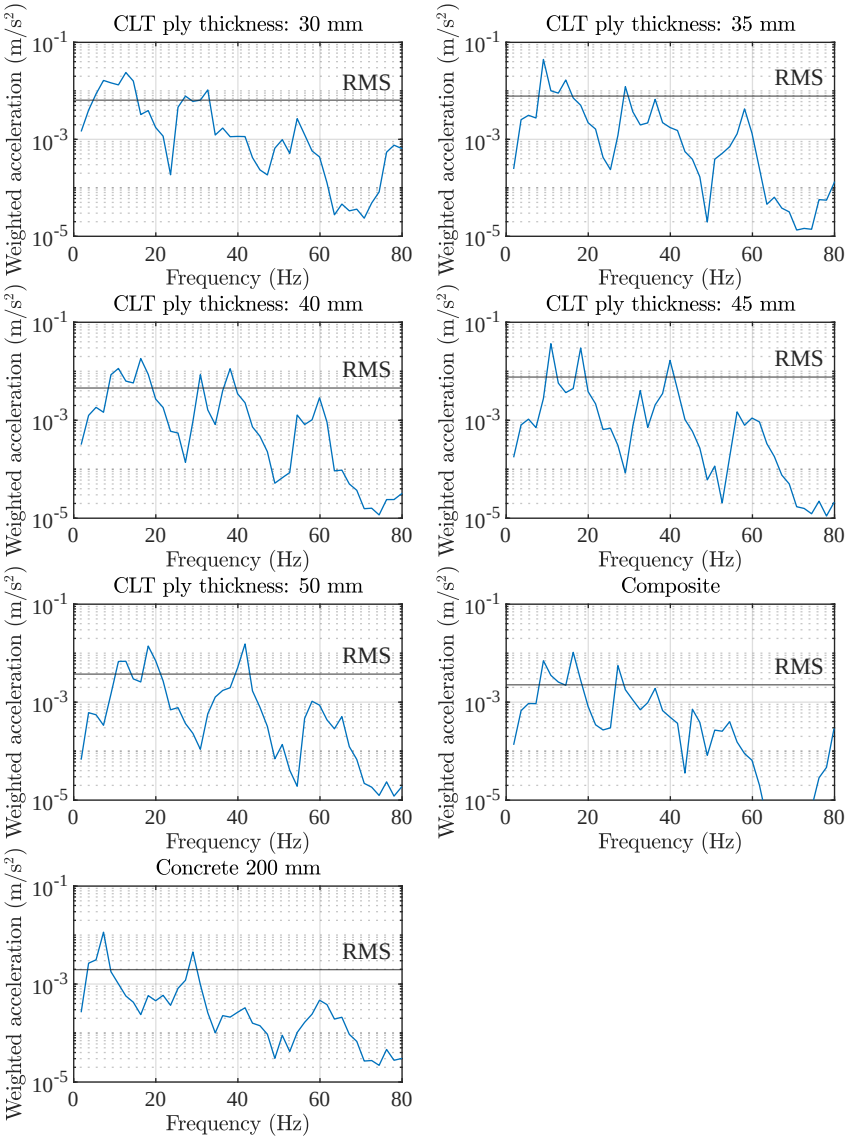

Figure A.1: Weighted frequency spectra for a footstep pulse with walking frequency 1.83 Hz.

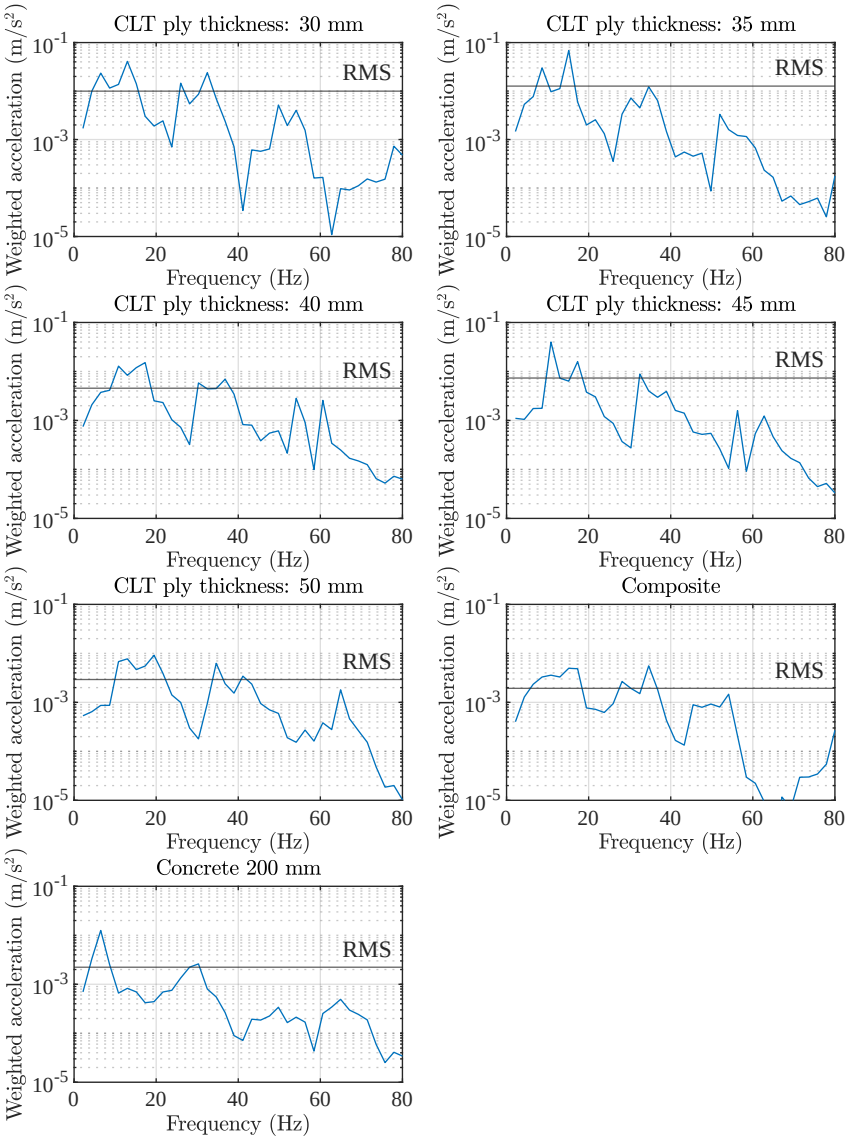

Figure A.2: Weighted frequency spectra for a footstep pulse with walking frequency 2.17 Hz.

Appendix B

Velocity of first and second floor

From the analysis of a building exposed to an external load, the velocities of the investigated buildings on the stiff soil in the first floor and the second floor are presented in Figure B.1 and Figure B.2.

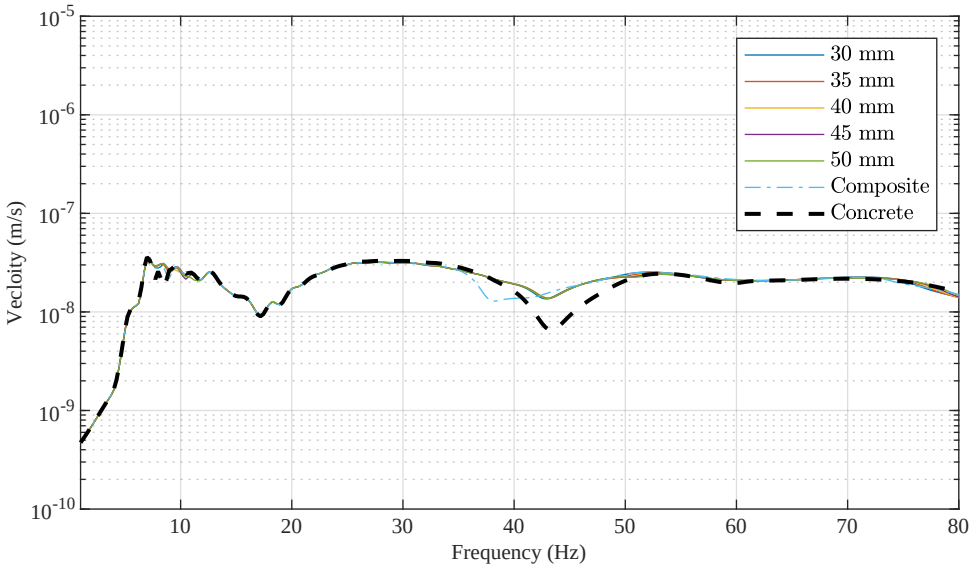

Figure B.1: Velocity of the first floor of the investigated buildings on the stiff soil.

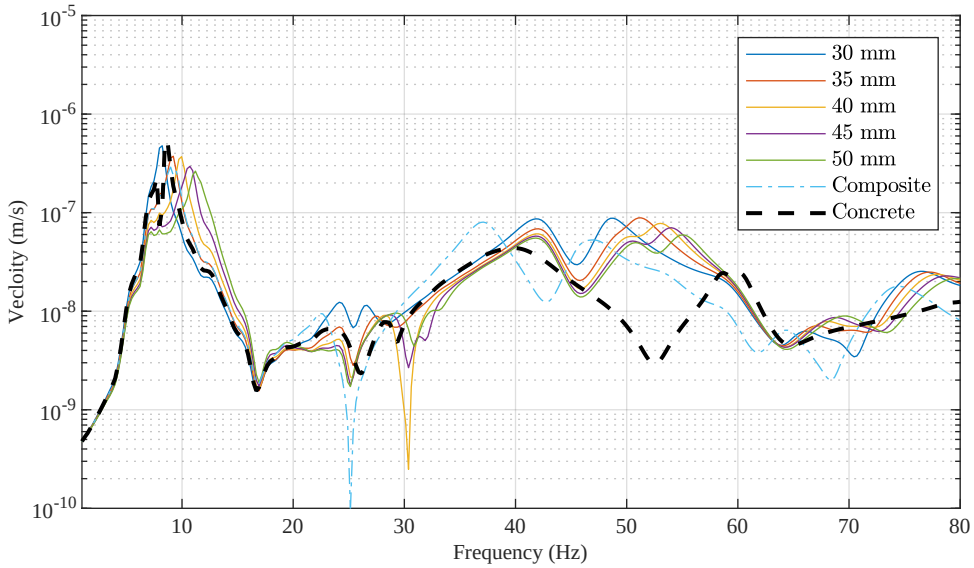

Figure B.2: Velocity of the second floor of the investigated buildings on the stiff soil.

Presented in Figure B.3 and Figure B.4 are the velocities of the first floor and the second floor respectively of the investigated buildings on a soft soil.

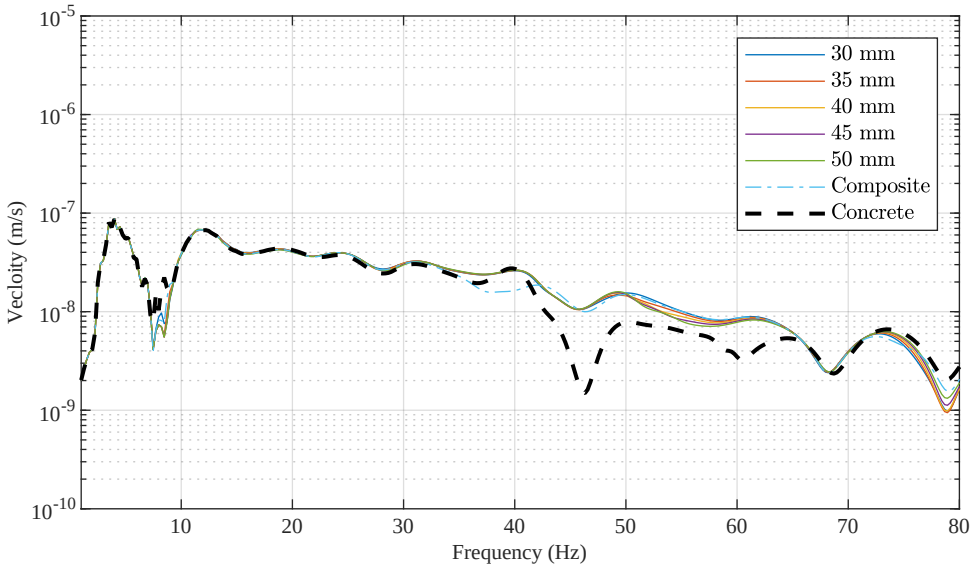

Figure B.3: Velocity of the first floor of the investigated buildings on a soft soil.

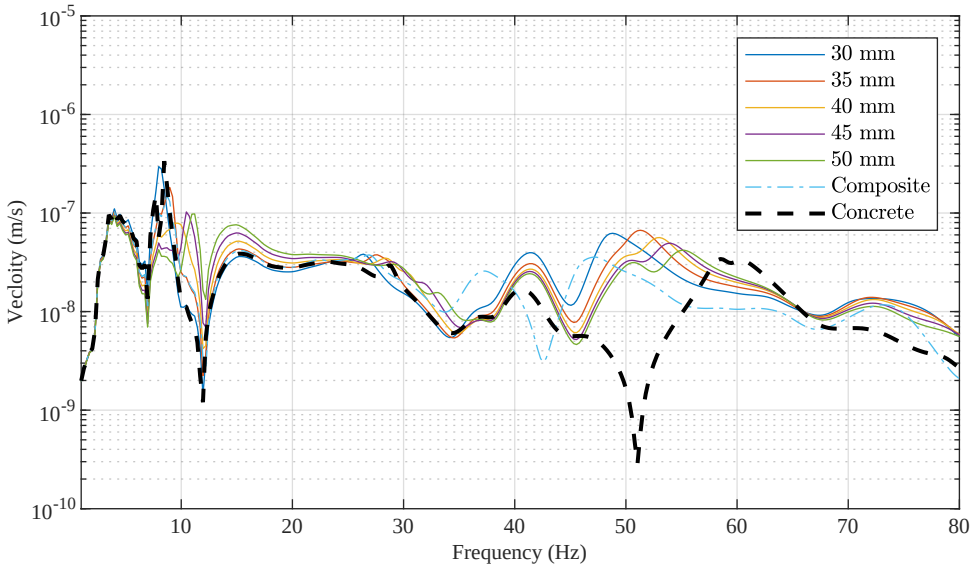

Figure B.4: Velocity of the second floor of the investigated buildings on a stiff soil.